Volume 128 Issues 1-4 February 1, 2012 ISSN 0169-7722

JOURNAL OF
CONTAMINANT
HYDROLOGY

Editors

G.B. Davis, CSIRO Land and Water
S.B. Haderlein, University of Tübingen, Center for Applied Geoscience
D.A. Sabatini, University of Oklahoma, School of Civil Engineering and Environmental Science
B.E. Sleep, University of Toronto, Department of Civil Engineering

(This is a sample cover image for this issue. The actual cover is not yet available at this time.)

Cyclic biogeochemical processes and nitrogen fate beneath a subtropical stormwater infiltration basin

Andrew M. O'Reilly [a], Ni-Bin Chang [b,*], Martin P. Wanielista [c]

[a] U.S. Geological Survey, Florida Water Science Center, 12703 Research Pkwy, Orlando, FL 32826, USA
[b] University of Central Florida, Department of Civil, Environmental, and Construction Engineering, 4000 Central Florida Blvd, Building 91, Suite 442, Orlando, FL 32816, USA
[c] University of Central Florida, Water Research Center and Stormwater Management Academy, 4000 Central Florida Blvd, Building 91, Suite 442, Orlando, FL 32816, USA

ARTICLE INFO

ABSTRACT

A stormwater infiltration basin in north–central Florida, USA, was monitored from 2007 through 2008 to identify subsurface biogeochemical processes, with emphasis on N cycling, under the highly variable hydrologic conditions common in humid, subtropical climates. Cyclic variations in biogeochemical processes generally coincided with wet and dry hydrologic conditions. Oxidizing conditions in the subsurface persisted for about one month or less at the beginning of wet periods with dissolved O_2 and NO_3^- showing similar temporal patterns. Reducing conditions in the subsurface evolved during prolonged flooding of the basin. At about the same time O_2 and NO_3^- reduction concluded, Mn, Fe and SO_4^{2-} reduction began, with the onset of methanogenesis one month later. Reducing conditions persisted up to six months, continuing into subsequent dry periods until the next major oxidizing infiltration event. Evidence of denitrification in shallow groundwater at the site is supported by median NO_3^-–N less than 0.016 mg L^{-1}, excess N_2 up to 3 mg L^{-1} progressively enriched in $\delta^{15}N$ during prolonged basin flooding, and isotopically heavy $\delta^{15}N$ and $\delta^{18}O$ of NO_3^- (up to 25‰ and 15‰, respectively). Isotopic enrichment of newly infiltrated stormwater suggests denitrification was partially completed within two days. Soil and water chemistry data suggest that a biogeochemically active zone exists in the upper 1.4 m of soil, where organic carbon was the likely electron donor supplied by organic matter in soil solids or dissolved in infiltrating stormwater. The cyclic nature of reducing conditions effectively controlled the N cycle, switching N fate beneath the basin from NO_3^- leaching to reduction in the shallow saturated zone. Results can inform design of functionalized soil amendments that could replace the native soil in a stormwater infiltration basin and mitigate potential NO_3^- leaching to groundwater by replicating the biogeochemical conditions under the observed basin.

1. Introduction

As the demand for fresh water increases worldwide, stormwater is increasingly being managed as a resource by operation of stormwater infiltration basins to supplement aquifer recharge or to augment groundwater quantity for subsequent withdrawal by harvesting of infiltrated stormwater (Clark and Pitt, 2007; Page et al., 2010). Traditionally, stormwater has been managed from the perspective of surface-water impacts, but more recently there has been a focus on groundwater impacts (Fisher et al., 2003; Hatt et

al., 2009; Pitt et al., 1999). Taylor et al. (2005) suggest that an important area for future stormwater treatment research is improved best management practices (BMPs) to mitigate nitrogen (N) species in stormwater, especially enhancing dissolved N treatment. However, the highly dynamic nature of infiltrated water and groundwater beneath infiltration basins complicates understanding of an already complex biogeochemical system (Cho et al., 2009; Datry et al., 2004). Little research at the field scale is available on the temporal variability of N cycling beneath stormwater infiltration basins.

The most common N species of concern is nitrate (NO_3^-), due to its worldwide prevalence in surface water and groundwater and potential human health impacts (Vitousek et al., 1997; Ward et al., 2005). Stormwater runoff is one of many sources of N (Kim et al., 2003; Page et al., 2010; Schiffer, 1989; Taylor et al., 2005), among others such as septic tanks (Katz et al., 2010) and land-based application of reclaimed water (Sumner and Bradner, 1996) or fertilizer (Böhlke, 2002; Green et al., 2008a), which can contribute to elevated NO_3^- concentrations in groundwater. Nitrogen, particularly NO_3^-, easily moves from terrestrial ecosystems into groundwater and surface waters (Baker, 1992; Kahl et al., 1993; Peterjohn et al., 1996).

Because N often is the limiting nutrient for plants (Einsle and Kroneck, 2004), increased quantities of N in ecosystems alter competitive relationships among terrestrial and aquatic organisms (U.S. Environmental Protection Agency, 2005). Elevated NO_3^-–nitrogen (NO_3^-–N) concentrations exceeding $0.1 \, mg \, L^{-1}$, a level representative of background conditions in the Upper Floridan aquifer in Florida (Katz, 1992; Maddox et al., 1992), are common in Florida groundwater (O'Reilly et al., 2007). Consequently, NO_3^-–N concentrations have increased in many springs since the 1950s, exceeding $1 \, mg \, L^{-1}$ in recent years at some springs in central and north Florida (Katz, 2004; Katz et al., 1999, 2009; Knowles et al., 2010; Phelps, 2004; Phelps et al., 2006; St. Johns River Water Management District, 2010). Walsh et al. (2009, p. 89) state that "increased nutrient input to Florida springs is the single greatest threat to the ecology of these systems." In recognition of these factors, a NO_3^-–N (plus nitrite) of $0.35 \, mg \, L^{-1}$ was recently proposed as a protective criterion for aquatic life in Florida's springs and clear streams (U.S. Environmental Protection Agency, 2011).

Due to the episodic nature of stormwater runoff generation and the large volume of water accumulated by stormwater conveyance systems in urban and suburban settings, infiltration and groundwater recharge processes beneath a stormwater infiltration basin can occur rapidly depending on the hydrogeologic conditions (Cho et al., 2009; Professional Service Industries, Inc., 1993) and a substantial amount of recharge can be contributed to underlying aquifers (Fisher et al., 2003; Zubair et al., 2010). These factors result in a highly dynamic shallow groundwater system beneath a stormwater infiltration basin that is continuously adjusting to changing inputs. These dynamics mediate the major processes controlling the occurrence of NO_3^- and other N species in groundwater that originate from stormwater infiltration: (1) advective transport of N into the aquifer (infiltration and percolation through the unsaturated zone); and (2) physical (particulate and colloidal straining), chemical (solid, aqueous and gas phase interactions) and biological (ammonification, nitrification, NO_3^- reduction, and assimilation) transformation of N

along the flow path. Datry et al. (2004) showed that such conditions result in fluctuations in shallow groundwater quality (less than 3 m below the water table) at small spatial (1 m) and temporal (1 d) scales below an infiltration basin in Lyon, France, where the water table was less than 1.2 m deep. Cho et al. (2009) demonstrate through laboratory column experiments simulating a bioretention BMP that N cycling (the net effects of sorption, nitrification and denitrification) during intermittent wetting (6 h) and drying (7 d) resulted in inorganic N removal efficiencies exceeding 95%. Subsurface water quality changes may occur at time scales different from those of the underlying physicochemical and biological processes in response to the net effects of conservative mixing, hydrodynamic dispersion and reaction kinetics of waters with different travel times, initial chemical compositions and reaction histories (Green et al., 2010). Therefore, cyclic variations in groundwater quality may occur at seasonal or shorter time scales caused by infiltration fluxes and chemistry that fluctuate at daily or shorter time scales, and the relative time scales of transport and transformation processes determine the ultimate fate of a solute (Gu et al., 2007). For example, reaction kinetics for denitrification can be fast, with denitrification rates varying up to an order of magnitude at subdaily time scales for soil cores obtained from agricultural fields before and after rainfall (Sexstone et al., 1985). Cyclic patterns of denitrification were reported in soils beneath agricultural fields recurring at monthly or shorter (Weitz et al., 2001) to seasonal frequency (Mahmood et al., 2005). Given the intermittent nature of wet–dry cycles during both stormwater infiltration and crop cultivation, similar cyclic biogeochemical processes might be expected to occur beneath stormwater infiltration basins. Wet–dry cycles over a range of time scales affect N cycling (Austin et al., 2004). However, biogeochemical cycling beneath stormwater infiltration basins is not well documented.

To better understand the effects of temporal variations in water fluxes and biogeochemical cycling in the context of stormwater infiltration, a comprehensive study was conducted from 2007 through 2010 to identify both the hydrologic conditions and the biogeochemical processes beneath two stormwater infiltration basins, which may impact groundwater resources in a humid, subtropical climate (O'Reilly et al., 2011). The objective of this paper is to elucidate the sequential biogeochemical processes occurring cyclically at seasonal or shorter time scales and demonstrate that such processes can effectively control N fate in this setting. Results focus on data collected in 2007–2008 at one stormwater infiltration basin where substantial biogeochemical cycling and N transformation were observed. At this site, cyclic variations between oxidizing and reducing conditions effectively act to switch NO_3^- fate between leaching and reduction. By providing increased understanding of temporal biogeochemical variability in dynamic environments, results can inform development of improved BMPs to mitigate NO_3^- impacts from stormwater infiltration basins.

2. Material and methods

2.1. Study site

A stormwater infiltration basin located in the Silver Springs springshed approximately 9 km southwest of Silver

Springs in north–central Florida, USA, was monitored during 2007–2008 to identify subsurface biogeochemical processes (Fig. 1). Silver Springs is a large group of springs (1933—2007 annual mean discharge was 21.7 $m^3 s^{-1}$; Knowles et al., 2010) of substantial environmental and recreational importance, which has experienced an increase in $NO_3^- –N$ from 0.1 $mg\,L^{-1}$ in 1956 to a maximum of 1.2 $mg\,L^{-1}$ in 2004 (Phelps et al., 2006). The springshed is characterized by karst topography consisting of predominantly internal drainage into closed depressions or diffuse seepage into highly permeable surficial sediments (Phelps, 2004). The climate of the area is humid subtropical, with hot, rainy summers and cool, relatively dry winters (Phelps, 2004). Long-term (1901–2008) annual averages indicate rainfall of about 1360 $mm\,yr^{-1}$ and mean daily air temperature of about 22 °C at the National Oceanic and Atmospheric Administration (NOAA) Ocala station (COOP ID 086414) approximately 7 km south of the stormwater basin (National Climate Data Center, 2011). Annual average rainfall was 1400 and 1130 $mm\,yr^{-1}$ in 2007 and 2008, respectively; minimum daily air temperature averaged about 15 °C; and maximum daily air temperature averaged about 28 °C. Potential evapotranspiration averaged about 1250 $mm\,yr^{-1}$ (1996–2009) based on daily values computed from GOES-satellite data and using the Priestley–Taylor
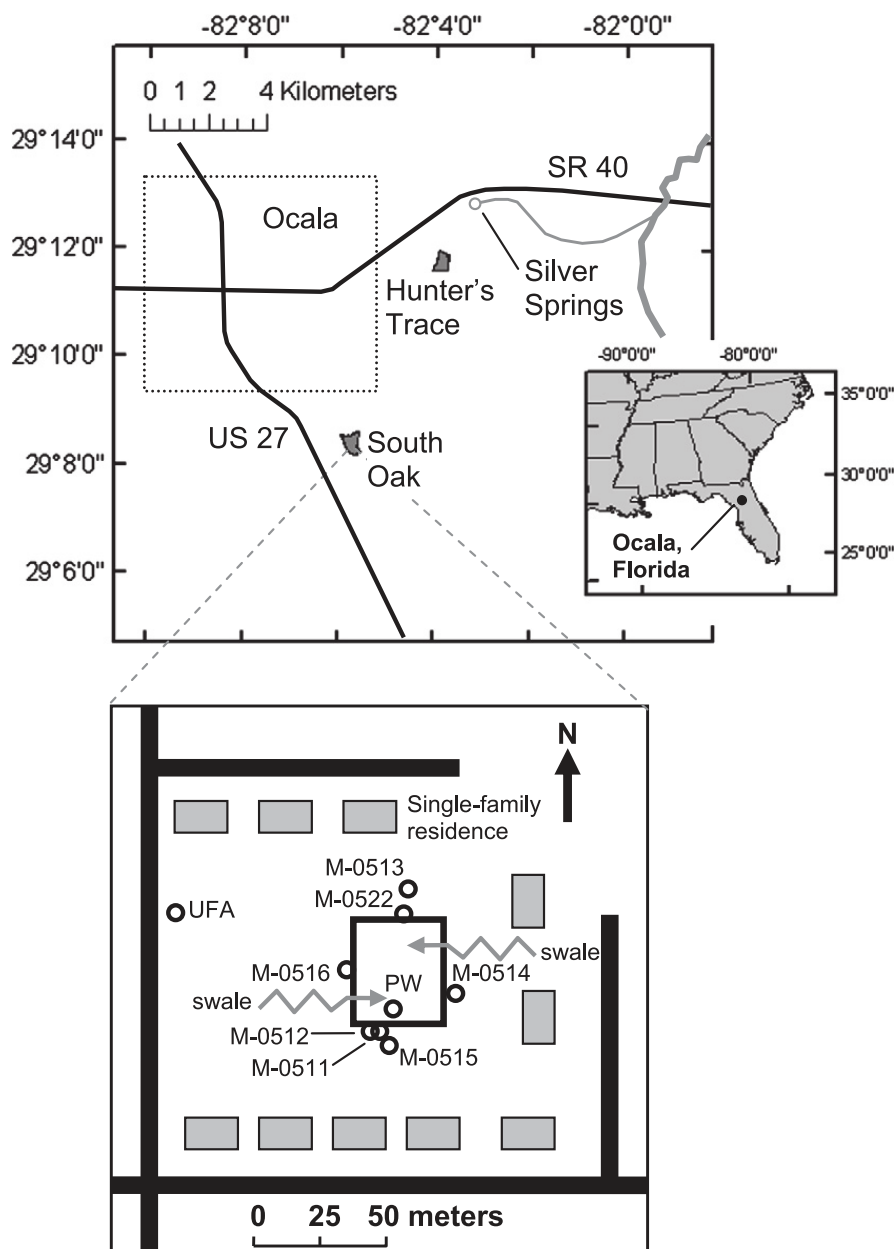
Fig. 1. Locations of the South Oak and Hunter's Trace stormwater infiltration basins. Upper map shows location of each watershed, and inset map shows the study area (South Oak site) with the locations of monitoring sites relative to the basin.

equation (Mecikalski et al., 2011) for a 2-km pixel covering the NOAA Ocala station (U.S. Geological Survey, 2011a,b).

North–central Florida is underlain by three principal hydrogeologic units in order from shallowest to deepest: (1) surficial aquifer system, consisting of varying amounts of sand, silt and clay; (2) intermediate confining unit, which is predominantly clay; and (3) Floridan aquifer system, which is a thick sequence of carbonate formations. The surficial aquifer system and intermediate confining unit correspond to the post-Miocene and Miocene sediments, respectively, and are thin and discontinuous (Phelps, 2004). The Floridan aquifer system comprises the Upper and Lower Floridan aquifers; the Upper Floridan aquifer is generally 90 m thick in north–central Florida and serves as the primary source of fresh water for numerous springs as well as for drinking water and irrigation purposes (Phelps, 2004). The top of the limestone at the study site is highly variable; limestone was found at a depth of 9.8 m at well M-0511 (Fig. 1) but was not present in a 15-m deep boring 30 m to the west (Andreyev Engineering, Inc., personal communication, 2007).

The South Oak stormwater infiltration basin that is the focus of this paper (Fig. 1) is located in a watershed that has transitioned from rural to residential land use during 1973–1990 and remains residential as of 2011. The stormwater basin is 1600 m^2 in area with a watershed of 29 ha, and functions to infiltrate stored water without surface outlets. In 1973, land use in the watershed draining to the basin was approximately 80% agricultural (nursery, specialty crops and citrus) and 20% hardwood forest. In 2004, land use in the watershed was approximately 70% low-density residential and 30% medium-density residential. Soils in the watershed are predominantly well drained (hydrologic group A) and consist of Hague sand, Kanapaha fine sand and Kendrick loamy sand (Thomas et al., 1979). Soils in the immediate vicinity of the basin are considerably finer-textured and poorly drained compared to those of its watershed. Fine-textured sediments just beneath the bottom of the basin effectively represent the intermediate confining unit, thus the surficial aquifer system is thin or absent at the site. The stormwater basin occupies a natural land-surface depression and was excavated to a depth of about 1 m. Although the basin overflows the excavated basin boundaries during prolonged or intense storm events, it remains confined to the larger natural depression. Roadside swales are the primary system used to convey runoff to the stormwater basin. Impervious area attributable to roadways is estimated to be 5% of the watershed.

2.2. Hydrologic monitoring

Hydrologic monitoring consisted of measurements of rainfall, basin stage (stored stormwater level), groundwater level, subsurface temperature, and volumetric soil moisture content. Rainfall was measured with a siphon-type tipping bucket gage (TR-525S, Texas Electronics, Inc., Dallas, TX[1]), basin stage and groundwater level were measured with

submersible pressure transducers (MPSDIT.010, vented and temperature compensated, Rittmeyer Ltd., Zug, Switzerland), temperature was measured using thermistors, and volumetric soil moisture content was measured using time domain reflectometry (TDR). TDR measurements were adjusted, as necessary, based on gravimetric measurement of volumetric moisture content on undisturbed soil cores at field and saturated moisture contents. Continuous data were recorded at 5-minute intervals from December 2007 through December 2009. Periodic (approximately monthly) measurements of basin stage and groundwater level were made March–December 2007.

Monitoring wells were installed by hollow-stem auger in March 2007 (Fig. 1). The wells consisted of a 5.1-cm-diameter PVC casing with a 1.5-m-length screen. Wells depths were less than 3 m below the water table with the exception of well M-0511, which was approximately 6 m deeper. Only water level and temperature data were collected at well M-0511 because low water yield from fine-textured sediments precluded collection of representative water samples. Suction lysimeters with a 20-cm-long porous cup (model 1923, Soilmoisture Equipment Corporation, Santa Barbara, CA) were installed at each site by hand excavation at depths of 0.5, 0.9 and 1.4 m adjacent to well PW inside the basin. To minimize preferential flow paths, the porous cups of the lysimeters were embedded in a silica flour and deionized water slurry, overlain by a 15-cm-thick layer of bentonite chips subsequently hydrated with deionized water, and backfilled to land surface in layers with careful tamping using native soil. TDR and thermistor probes (CS616-L and 107-L, respectively, Campbell Scientific, Inc., Logan, UT) were installed adjacent to the lysimeters by hand excavation and inserted horizontally into the undisturbed excavation wall at depths of 0.3, 0.6 and 0.9 m.

2.3. Soil chemistry

Nineteen soil samples for analysis of carbon (C) and N content were collected during four sampling events from March to December 2008, representing a variety of hydrologic conditions. Samples were collected by hand auger or double-cylinder hammer-driven core sampler (Grossman and Reinsch, 2002), placed in 500 mL polyethylene widemouth bottles, packed in ice in the field, and subsequently stored frozen until analysis. Soil samples were collected for each sampling event from a single borehole within 3 m of well PW at depths from 0.1 to 2.3 m (Fig. 1); each borehole was backfilled to land surface in layers with careful tamping using native soil. Soil solids were analyzed for organic carbon (OC) according to procedures outlined by Walkley and Black (1934) and total carbon (TC) and total nitrogen (TN) by combustion–oxidation (Shimadzu TOC-V/SSM-5000A, Shimadzu Scientific Instruments, Columbia, MD). Inorganic carbon (IC) was computed as the difference between TC and OC. Two extractions were performed for each sample, one using 2 M potassium chloride (KCl) and one using distilled water. Both KCl and water solutions were then analyzed for NH_4^+ (EPA Method 350.1), NO_3^- plus NO_2^- (EPA Method 353.2), and NO_3^- (UV spectrophotometry, Norman and Stucki, 1981); water solutions were additionally analyzed for OC, TC and TN by combustion–oxidation (Shimadzu TOC-V/CPH/CPN, Shimadzu

---

[1] Any use of trade, firm, or product names is for descriptive purposes only and does not imply endorsement by the U.S. Government.

Scientific Instruments, Columbia, MD). Inorganic N (IN) was computed as the sum of NH_4^+, NO_3^- and NO_2^-; organic N (ON) was computed as the difference between TN and IN. The KCl-soil solutions were shaken for 1 h on a reciprocating shaker to provide an estimate of concentrations based on analyte mass both adsorbed to soil particles and dissolved in soil pore water. The water solution extractions were incubated without agitation for 48 h at 4 °C (to minimize microbial activity) before extraction to provide an estimate of analyte mass in soil pore water as well as mass that might be more loosely sorbed to soil particles. The C and N concentrations in the sample/water-solution mixtures were presumed equilibrated after incubation. Moisture content by drying at 105 °C was determined for each sample and used in the computation of final analyte concentration on a per mass basis for both extraction procedures. Soil chemical analyses were performed by the University of Florida Soil Core Laboratory in Gainesville, Florida (W.G. Harris, personal communication, 2009, 2010).

2.4. Water chemistry

Water samples were collected for chemical analysis of precipitation, stormwater, soil water and groundwater (June 2007–December 2008). Water samples were collected and processed following standard USGS protocol (U.S. Geological Survey, 1998). Monitoring wells were purged prior to each sampling event until at least three casing volumes of water were removed, and field properties (temperature, specific conductance, pH, dissolved oxygen (DO) and redox potential (E_h)) had stabilized. Field properties were measured for all water samples using a YSI 556MPS multi-parameter sonde (prior to May 2008) and YSI 6920 V2 multi-parameter sonde (May 2008 and later) (YSI Incorporated, Yellow Springs, OH); a flow-through chamber was used for groundwater samples. Sondes were calibrated daily against known standards according to standard USGS protocols (Wilde and Radtke, 1998). When water was stored in the basin, stormwater samples were collected at five locations within the basin (by wading) by filling a 1 L amber glass bottle (precombusted at 450 °C) through the full depth of standing water and compositing by churn. Stormwater field properties (temperature, specific conductance, pH, DO and E_h) were measured at the same five locations and median values reported. Stormwater samples were collected under generally different conditions, including during a rain event and basin filling, when the basin was full, and near the end of extended flooding events. Soil–water samples were collected by first purging the lysimeter and then applying a pressure of −60 kPa and allowing the lysimeter to fill for 6–48 h, depending on the ambient soil moisture content. Atmospheric air was then used to apply a pressure to force the water from the lysimeter into a 1 L amber glass bottle (precombusted at 450 °C) from which water was withdrawn by peristaltic pump for filtration and bottle filling. Field properties (temperature, specific conductance and pH only) for soil–water samples were measured using a subsample from the 1 L bottle collected immediately after filling. A precipitation (bulk deposition) sample was obtained by collection in an 8 L plastic bucket from which water was withdrawn by peristaltic pump for filtration and bottle filling. Alkalinity

was determined for all samples by incremental titration with 0.16 N or 1.6 N sulfuric acid.

Water samples were collected for laboratory analysis of major ions, trace elements, nutrients and organic carbon. Major ions included Ca^{2+}, K^+, Mg^{2+}, Na^+, Br^-, Cl^-, F^-, SO_4^{2-}, Si and alkalinity. Trace elements and nutrients included Al, B, Cd, Co, Cr, Cu, Fe, Mn, Mo, Ni, Pb, Se, V, W and Zn. Nutrients included NH_4^+ as N, NO_3^- plus NO_2^- as N, NO_2^- as N, TN, orthophosphate as P, and total P. Organic carbon samples included total organic carbon (TOC) and dissolved organic carbon (DOC).

Samples collected for analyses of major ions, trace elements, and nutrients were filtered through a 0.45-μm pore-size disposable encapsulated filter, rinsed with deionized and sample water. DOC samples were filtered through 0.45-μm pore-size disposable encapsulated filter, rinsed with water certified to be free of organic carbon and with sample water. Filtered samples for all analytes were collected for precipitation, soil water, and groundwater and unfiltered samples for TN and total P were collected for groundwater samples; both filtered and unfiltered samples for all analytes were collected for stormwater. All major ion, trace element, nutrient, and organic carbon samples were analyzed by the USGS National Water-Quality Laboratory in Denver, Colorado, using previously documented methods (Brenton and Arnett, 1993; Clesceri et al., 1998; Fishman, 1993; Fishman and Friedman, 1989; Garbarino and Struzeski, 1998; Garbarino et al., 2006; Hoffman et al., 1996; Patton and Kryskalla, 2003; Struzeski et al., 1996).

2.5. Dissolved gasses

Measurement of DO in groundwater and basin stormwater was performed in the field using a polarographic sensor (YSI 556MPS) from June 2007 to April 2008 and an optical sensor (YSI 6920 V2) from May 2008 to December 2008 (YSI Incorporated, Yellow Springs, OH). Groundwater samples collected between March and December 2008 were also analyzed for major dissolved gasses (Ar, N_2, O_2, CO_2, CH_4) by gas chromatography (GC) by the USGS Chlorofluorocarbon Laboratory in Reston, Virginia (Busenberg et al., 2001). Duplicate dissolved gas samples were collected in 160 mL serum bottles that were filled gently overflowing from the bottom while submerged in a larger container. When full, a thick butyl rubber stopper was inserted into the bottle with a syringe needle in place to permit excess water to escape. Samples were preserved by packing bottles in ice in the field and storing at 0–4 °C until analysis (Böhlke et al., 2004). Lack of KOH preservation can allow microbial activity in the sample bottle to affect biogenic gas concentrations (P.K. Widman, personal communication, 2009). The primary analytes of interest are Ar and N_2 (from which excess N_2 attributable to denitrification can be estimated). Groundwater generally had low O_2 and NO_3^- concentrations, therefore nitrification/denitrification reactions in the sample bottles likely were minimal. CO_2 and CH_4 concentrations possibly could have been affected and were therefore interpreted qualitatively. Analysis of duplicate bottles indicated 2-sigma (σ) coefficients of variations for Ar, N_2, CO_2 and CH_4 of 0.4%, 0.5%, 1.4% and 1.7%, respectively. Large variations in GC-derived O_2 concentrations were noted, therefore only field measured O_2 concentrations were used.

2.6. Stable isotopes of nitrogen and oxygen

Isotopic values are reported using standard delta (δ) notation (Clark and Fritz, 1997) as follows: $\delta R_{sample} = [(R_{sample}/R_{standard}) - 1] \times 1000$. For $\delta^{15}N$, $R = {}^{15}N/{}^{14}N$; and for $\delta^{18}O$, $R = {}^{18}O/{}^{16}O$. Results are reported in parts per thousand (per mil, ‰). N isotopes are reported relative to N_2 in air (Mariotti, 1983), and O isotopes are reported relative to Vienna Standard Mean Ocean Water (Coplen, 1988; Coplen, 1994). $\delta^{15}N$ values were measured for NO_3^- and dissolved N_2, and $\delta^{18}O$ values were measured for NO_3^- and H_2O for samples collected March 2008 to December 2008. NO_3^- samples for isotopic analysis were collected in opaque polyethylene bottles after filtration (0.45-μm pore-size disposable encapsulated filter), packed in ice in the field, and subsequently frozen until analysis. NO_3^- samples were analyzed by bacterial conversion of NO_3^- to nitrous oxide and subsequent measurement on a continuous flow isotope ratio mass spectrometer (Casciotti et al., 2002; Coplen et al., 2004; Révész and Casciotti, 2007; Sigman et al., 2001). For samples with NO_3^-–N of at least 0.06 mg kg^{-1}, the 2σ uncertainty of N and O isotopic results is 0.5‰ and 1‰, respectively. For NO_3^-–N less than 0.06 mg kg^{-1}, the 2σ uncertainty of N and O isotopic results is 1‰ and 2‰, respectively. H_2O samples for isotopic analysis were collected in glass bottles after filtration with 0.45-μm pore-size disposable encapsulated filter. $\delta^{18}O$ was determined using the CO_2 equilibration technique (Epstein and Mayeda, 1953; Révész and Coplen, 2008) with 2σ uncertainty of 0.2‰. Isotopic analysis of NO_3^- and H_2O samples was performed by the USGS Reston Stable Isotope Laboratory in Reston, Virginia. Isotopic analysis of N_2 samples was performed on 160 mL serum bottle headspace after GC gas concentration analysis (Section 2.5) on an isotope ratio mass spectrometer (Tobias et al., 2007) at the USGS laboratory in Reston, Virginia, under the direction of J.K. Böhlke. $\delta^{15}N[N_2]$ measurements were calibrated by analyzing air-equilibrated water standards prepared the same way as the samples. Replicate analyses of environmental samples and air-saturated water typically had reproducibility of ± 0.1‰ or less.

3. Results and discussion

3.1. Hydrologic conditions

The 5-minute hydrologic monitoring data were composited into daily values (summed for rainfall and averaged for all other values) for 2008–2009 (Fig. 2). An additional year of hydrologic monitoring was performed in 2009, even though no sampling occurred, in order to better characterize temporal variability. Annual rainfall was close to the long-term average and similarly distributed in time during the two years. During the period of water-quality sampling (June 2007–December 2008), the basin was flooded 68% of the time; on an annual basis, the basin was flooded 61% and 48% of the time in 2008 and 2009, respectively. The longest flooding periods began during the summer wet season and extended into early autumn (Fig. 2B). The greater percentage of flooding in 2008 is due to a particularly large rainfall event (155 mm from Tropical Storm Fay) that occurred in August, resulting in a greater depth of flooding compared to more
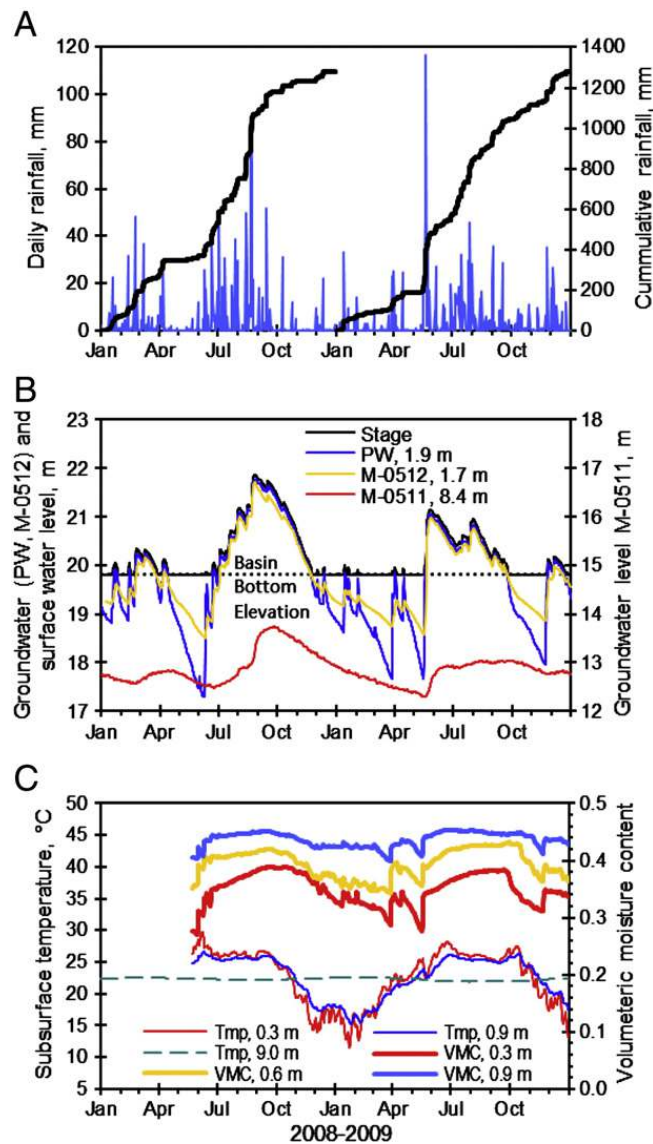

Fig. 2. Hydrologic monitoring of (A) rainfall, (B) basin stage and groundwater level, and (C) volumetric moisture content (VMC) and subsurface temperature (Tmp). Mid-screen depths of wells noted for groundwater level, and probe depths noted for VMC and Tmp.

typical rainfall periods. Infiltration rates were estimated by analysis of basin stage recession curves for several storm events in 2008. For 46–155 mm rainfall events (5–33 h duration), infiltration rates were 14–29 mm d^{-1}.

A comparison of basin volume and storm magnitude (rainfall depth) suggests that the majority of the watershed does not contribute runoff to the basin, except perhaps during extreme, prolonged storm events. For example during Tropical Storm Fay, 155 mm of rainfall occurred during a 33-h period causing a rainfall excess of about 36 mm based on the curve number method and a weighted curve number of 53 derived from land use and soil hydrologic group (Wanielista et al., 1997). The resulting 0.6-m rise in water stored in the basin suggests that only about 17% of the rainfall excess volume was contributing runoff to the basin. Considering that impervious areas cover a small portion of the watershed yet runoff depth from impervious areas will be disproportionately greater than pervious areas, the actual

area of the watershed contributing runoff probably is substantially smaller than 17%. These results are consistent with the karst, well-drained terrain of the watershed.

The response of the measured hydrologic variables to rainfall and air temperature indicates a subdued response with depth. The highly attenuated response of well M-0511 (Fig. 2B) is attributable to a prevalence of fine-textured sediments. Substantial silt and clay generally are present throughout the soil profile (Fig. 3A). Visual observation of split-spoon samples from wells outside the perimeter of the basin (Fig. 1) indicates that lithology varies across the site compared to that beneath the basin (Fig. 3A) but still indicates an abundance of silt and clay sediments. These fine-textured sediments cause large vertical head gradients of 0.90–1.3 mm^{-1} between M-0511 (9.1 m deep) and M-0512 (2.5 m deep). The two shallow wells inside or at the edge of the typical stored stormwater area (PW and M-0512, Fig. 1) respond rapidly to runoff events; subsequently, water percolates slowly through the sandy silts and clays leading to an attenuated response in well M-0511 (Fig. 2B). The nearly constant temperature signal (ranged from 21.9 to 22.5 °C) at a depth of 9 m (measured in M-0511, Fig. 2C) further illustrates the attenuating effects of the fine-textured sediments, and is near the long-term average air temperature of 22 °C.
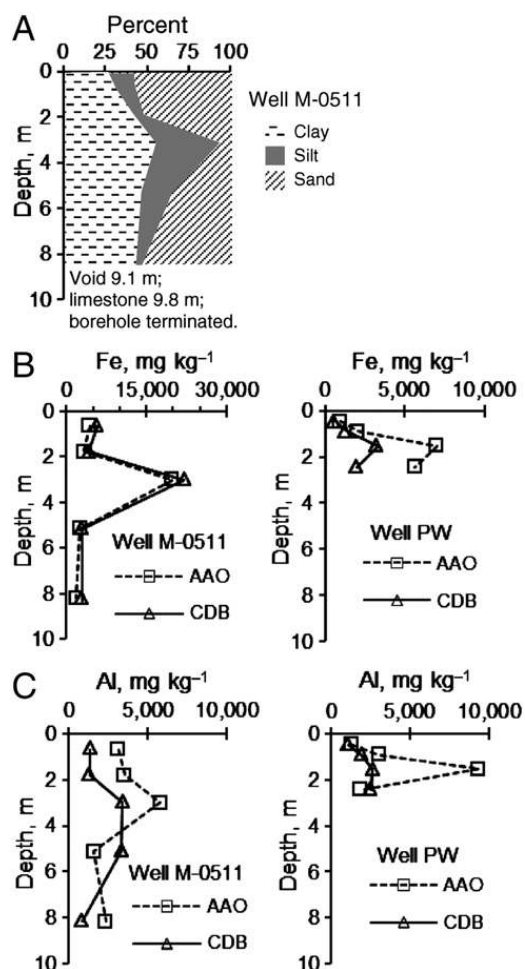

Fig. 3. Soil properties beneath the stormwater infiltration basin (A) texture profile; and (B) acid-ammonium-oxalate (AAO) and citrate-dithionite-bicarbonate (CDB) extractions of iron and aluminum oxides (Wanielista et al., 2011).

Lateral water-table gradients beneath the basin were both inward and outward from well PW within the basin to wells outside the perimeter of the basin (M-0512, M-0514, M-0515, M-0516 and M-0522; Fig. 1), ranging from −0.10 to 0.080 mm^{-1} (negative values inward, positive values outward). During periods of basin flooding, lateral gradients were always outward; whereas during dry periods, lateral gradients generally were inward (compare PW and M-0512 groundwater levels, Fig. 2B). Vertical head gradients (between the shallow wells and well M-0511) were always downward and were 30–600 times greater than lateral gradients. Assuming a vertical anisotropy of less than 10, which is typical of sandy sediments in central Florida (O'Reilly, 1998) and consistent with a single measurement at this site (Andreyev Engineering, Inc., personal communication, 2007), these gradients suggest that groundwater movement was predominantly downward beneath the basin.

Estimated horizontal and vertical pore-water velocities illustrate important implications for solute transport. Based on daily water-level measurements for wells PW and M-0512 (Fig. 2B), 10%, 50% and 90% exceedance probabilities corresponded to horizontal gradients of 0.018, 0.0035 and −0.065 mm^{-1} and vertical gradients of 0.068, 0.053 and 0.046 mm^{-1}, respectively. Based on applying Darcy's Law with a maximum hydraulic conductivity of 0.34 md^{-1} and an average porosity of 0.40 reported by Naujock (2008), the maximum horizontal pore-water velocity was 0.003 md^{-1} for the median measured gradient. Likewise, the maximum vertical pore-water velocity was 0.045 md^{-1} for the median measured gradient. Hydraulic conductivity values less than 0.02 md^{-1} at depths between 0.6 and 1.4 m (Naujock, 2008) likely control vertical percolation, thus Darcian-derived median vertical pore-water velocity was probably less than 0.004 mm d^{-1}. In contrast, based on infiltration rate estimates and a porosity of 0.40, vertical pore-water velocity ranged from 0.035 to 0.073 md^{-1}. The apparent discrepancy between pore-water velocities derived from Darcian and flooded infiltration methods is probably attributable to well-developed macropore structure observed in the fine-textured soils at the site, suggesting that much of the vertical water flux is through preferential flow paths. Consequently, solute transport behavior derived by Darcian analyses in such structured soils should be interpreted cautiously, with explicit accounting of macropore and soil matrix interaction leading to more accurate analyses (Arora et al., 2011).

3.2. Stormwater quality

Stormwater runoff into the basin brings infiltration of oxygenated water with elevated N concentrations (Fig. 4A), and at times results in substantial and prolonged water storage (Fig. 2B). Basin stormwater (water temporarily stored in the basin) had DO concentrations of 4.3–11 mg L^{-1} (median = 7.6 mg L^{-1}, n = 6) excluding the prolonged flooding event of 2008. During the prolonged flooding of 2008, DO of the stormwater was much lower (2.8, 0.4 and 1.7 mg L^{-1} for July, August and September, respectively) likely due to biochemical processes in the stormwater possibly related to the greater depth of water (frequently greater than 1 m). DO during the prolonged flooding of 2007 was higher (4.3 and 5.6 mg L^{-1}) possibly related to the shallower water
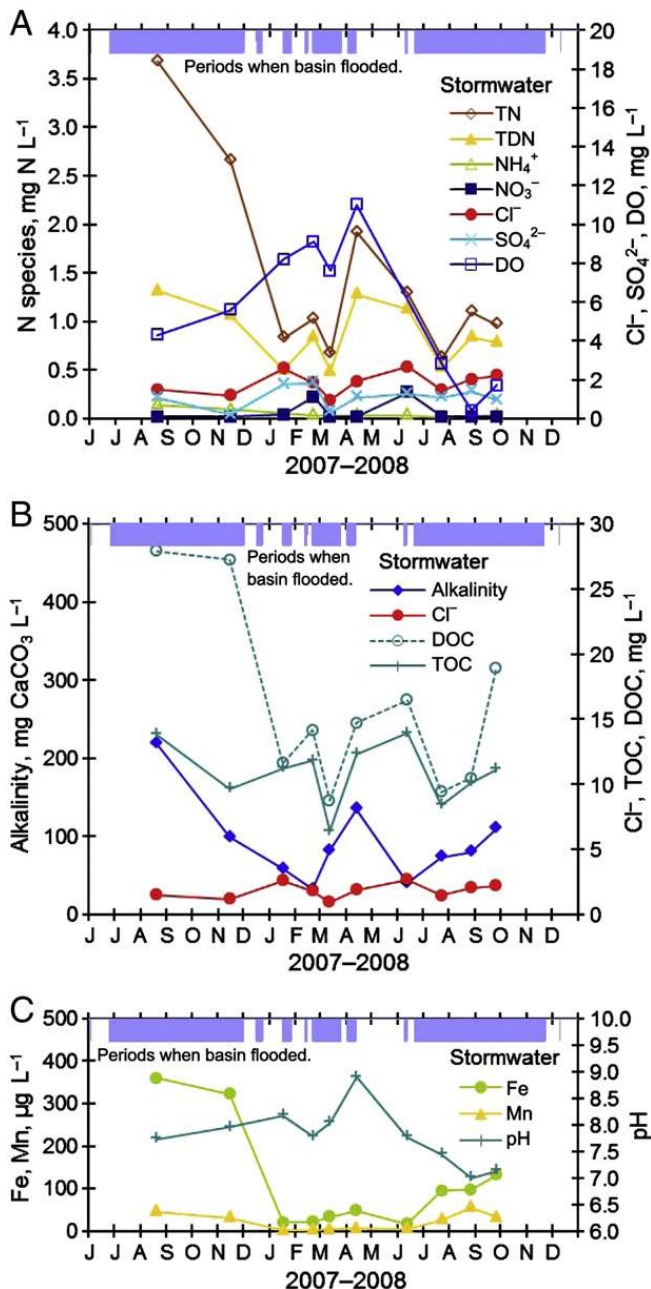
Fig. 4. Temporal variations in stormwater quality (A) nitrogen species, chloride, sulfate and dissolved oxygen; (B) DOC and alkalinity; and (C) iron, manganese and pH. Nitrogen species concentrations that did not exceed method detection limits are plotted at values equal to the laboratory reporting level (NH_4^+–N = 0.02 mg L^{-1}, NO_3^-–N = 0.016 mg L^{-1}). DOC, dissolved organic carbon; DO, dissolved oxygen; TDN, total dissolved nitrogen; TN, total nitrogen; TOC, total organic carbon.

depth (typically less than 0.5 m; basin stage estimated by periodic observations in 2007). OC content of the basin stormwater probably was increased by periodic submergence and decomposition of herbaceous vegetation that quickly grew during periods when the basin was not flooded. TOC concentrations ranged from 8.8 to 27.9 mg L^{-1} (median = 14.4 mg L^{-1}, n = 10) and was predominantly DOC (6.4–13.9 mg L^{-1}, median = 11.2 mg L^{-1}, n = 10) (Fig. 4B). Basin stormwater had total dissolved N (TDN) concentrations of 0.49–1.3 mg L^{-1} (median = 0.84 mg L^{-1}, n = 10), which

was nearly all ON with concentrations of 0.46–1.2 mg L^{-1} (median = 0.75 mg L^{-1}, n = 10). Maximum NO_3^-–N and NH_4^+–N were only 0.26 and 0.14 mg L^{-1}, respectively. Particulate and colloidal N could be an important source of N loading at times; total unfiltered N (TN) concentrations of basin stormwater were 0.62–3.7 mg L^{-1} (median = 1.0 mg L^{-1}, n = 10).

3.3. Groundwater quality

Groundwater quality in well PW (screened depth 1.2–2.7 m) (Fig. 5) generally was substantially different from stormwater quality (Fig. 4). Short periods of aerobic groundwater (DO concentrations of 3.5, 1.7 and 3.8 mg L^{-1} in January, February and June 2008, respectively) occurred after infiltration of aerobic stormwater (Fig. 5A). Otherwise, groundwater commonly had low DO or was anoxic beneath the basin (DO varied 0.1–0.9 mg L^{-1}, median = 0.3 mg L^{-1}, n = 11). DOC varied from 4.1 to 6.3 mg L^{-1} (median = 5.5 mg L^{-1}, n = 9) (Fig. 5B), and constituted about 95% of TOC (based on two samples analyzed for both DOC and TOC; data not shown). TN was nearly equal to TDN in groundwater from well PW (median TN = 0.31 mg L^{-1}, n = 14; data not shown), suggesting the retention of particulate and colloidal N at the sediment–water interface or during infiltration through the unsaturated zone. Groundwater had TDN concentrations of 0.25–3.1 mg L^{-1} (median = 0.32 mg L^{-1}, n = 14), which was predominantly ON with concentrations of 0.20–0.34 mg L^{-1} (median = 0.29 mg L^{-1}, n = 14). During periods of elevated TDN, NO_3^-–N was the predominant species (2.7, 2.3 and 0.84 mg L^{-1} in January, February and June 2008, respectively), which also coincided with aerobic periods. During other sampling events, NO_3^-–N was typically below the laboratory method detection limit (0.008 mg L^{-1}) and was no higher than 0.17 mg L^{-1}. Maximum NH_4^+–N was 0.048 mg L^{-1}. Alkalinity varied from 190 to 450 mg L^{-1} as $CaCO_3$ (Fig. 5B), and was predominantly HCO_3^- given the measured pH range of 6.2–6.7 (Fig. 5C).

3.4. Surface and subsurface water quality interaction

Evolution of subsurface water quality along a flow path from infiltration to eventual discharge commonly is influenced by reduction/oxidation (redox) reactions (Postma et al., 1991). Table 1 lists redox reactions that may potentially be occurring at the study site. Reactions are categorized as to occurrence under generally aerobic or anoxic conditions in recognition of the significant impact of aerobic stormwater on groundwater chemistry.

Considerable variation (in depth and time) occurred in soil water and groundwater quality in the upper 1.4 m of soil as indicated by samples collected from the three lysimeters (Fig. 6). However, temporal variations in underlying groundwater quality in well PW were comparatively small (compare Cl^- in Figs. 5A and 6). In the case of a relatively nonreactive constituent such as Cl^-, these differences are attributable to the combined effects of preferential flow, mobile versus relatively immobile pore-space water (Coats and Smith, 1964; Green et al., 2005), transient sorption (Pachepsky et al., 1994), evapoconcentration, and hydrodynamic dispersion processes. It is likely that Cl^- concentrations in groundwater
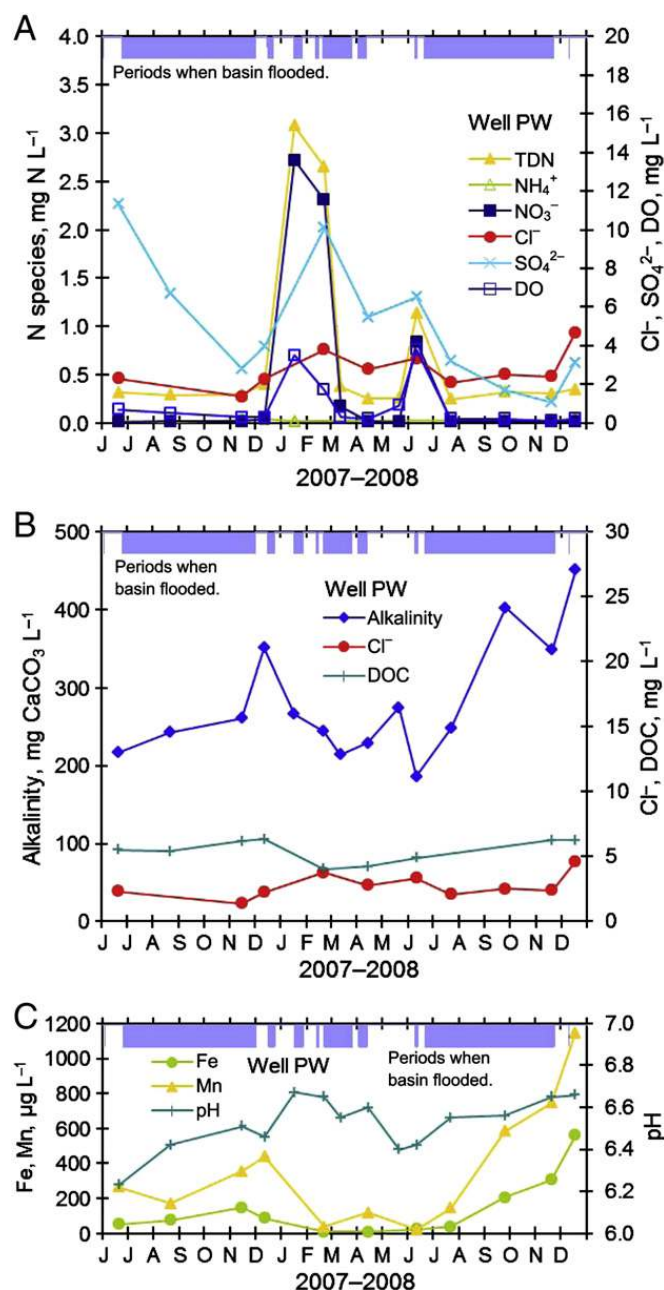
Fig. 5. Temporal variations in groundwater quality (well PW) (A) nitrogen species, chloride, sulfate and dissolved oxygen; (B) DOC and alkalinity; and (C) iron, manganese and pH. Nitrogen species concentrations that did not exceed method detection limits are plotted at values equal to the laboratory reporting level (NH_4^+–N = 0.02 mg L^{-1}, NO_3^-–N = 0.016 mg L^{-1}). DOC, dissolved organic carbon; DO, dissolved oxygen; TDN, total dissolved nitrogen.

from well PW are significantly influenced by preferential flow and mobile pore-space water and that concentrations in lysimeters are significantly influenced by the relatively immobile pore-space water and other physicochemical processes. For other more reactive constituents, such as redox sensitive DOC, TDN, Mn, Fe and SO_4^{2-}, geochemical and biogeochemical processes also are influential.

The net transformation of water quality during transition from stormwater to groundwater can be inferred by comparison of concurrent stormwater and groundwater samples. Ratios of groundwater to stormwater concentrations for redox sensitive constituents indicate variations considerably different to those of Cl^-, suggesting fate is reaction dominated (Supplemental Fig. S1). Thus, the physicochemical processes

controlling groundwater Cl^- concentrations play a lesser role in the fate of redox sensitive constituents. Accordingly, disparate patterns exist between Cl^- variations and the variation of each redox sensitive analyte for each lysimeter sample, with the exception of SO_4^{2-} (Fig. 6).

Temporal changes in SO_4^{2-} and Cl^- profiles suggest that physicochemical processes (sorption, evapoconcentration, and hydrodynamic dispersion) affect these anions in a similar fashion (Fig. 6; SO_4^{2-}/Cl^- ratios shown in Supplemental Fig. S2). To estimate the changes in SO_4^{2-} attributable to redox reactions, SO_4^{2-} concentrations were adjusted based on the percentage change in Cl^- concentrations between consecutive samples. One-third of the measured Cl^- percentage change was subtracted from the measured SO_4^{2-} percentage

Table 1

Reduction–oxidation reactions potentially occurring beneath the stormwater infiltration basin. The convention followed in the stoichiometric reactions is to show the electron donor as the first reactant and the electron acceptor as the second reactant. Electrons accepted is the number of electrons transferred in the reduction reaction. EA/ED ratio is the molar ratio of the electron acceptor to the electron donor based on the given stoichiometry adjusted to concentration units of mg L^{-1}, thus representing the decrease in the electron acceptor concentration via reduction by 1 mg L^{-1} of electron donor; DOC (represented by CH_2O) in mg C L^{-1}; all N species in mg N L^{-1}; Fe, Mn and S in solid phase reactants treated as equivalent concentration of dissociated ion. DNRA, dissimilatory nitrate reduction to ammonium.

Eq. No.	Biogeochemical process	Stoichiometry	Electrons accepted	EA/ED ratio
Aerobic conditions				
1	S$^-$ oxidation	$4FeS_{2(s)} + 15O_2 + 14H_2O \rightarrow 8SO_4^{2-} + 4Fe(OH)_{3(s)} + 16H^+$	S $\rightarrow$ O$_2$: 4	1.87
2	Fe(II) oxidation	$4Fe^{2+} + O_2 + 10H_2O \rightarrow 4Fe(OH)_{3(s)} + 8H^+$	Fe $\rightarrow$ O$_2$: 4	0.14
3	Mn(II) oxidation	$2Mn^{2+} + O_2 + 2H_2O \rightarrow 2MnO_{2(s)} + 4H^+$	Mn$\rightarrow$O$_2$: 4	0.29
4a	Nitrification	$2NH_4^+ + 3O_2 \rightarrow 2NO_2^- + 2H_2O + 4H^+$	N $\rightarrow$ O$_2$: 4	3.43
4b		$2NO_2^- + O_2 \rightarrow 2NO_3^-$	N $\rightarrow$ O$_2$: 4	1.14
5	Aerobic respiration	$CH_2O + O_2 \rightarrow CO_2 + H_2O$	C $\rightarrow$ O$_2$: 4	2.66
Anoxic conditions				
6	Heterotrophic denitrification	$5CH_2O + 4NO_3^- \rightarrow 2N_2 + 4HCO_3^- + CO_2 + 3H_2O$	C $\rightarrow$ N: 5	0.93
7	Autotrophic denitrification	$5Mn^{2+} + 2NO_3^- + 4H_2O \rightarrow N_2 + 5MnO_{2(s)} + 8H^+$	Mn $\rightarrow$ N: 5	0.10
8	Autotrophic denitrification	$10Fe^{2+} + 2NO_3^- + 14H_2O \rightarrow N_2 + 10FeOOH_{(s)} + 18H^+$	Fe $\rightarrow$ N: 5	0.050
9	Autotrophic denitrification	$5FeS_2 + 14NO_3^- + 4H^+ \rightarrow 7N_2 + 10SO_4^{2-} + 5Fe^{2+} + 2H_2O$	S $\rightarrow$ N: 5	0.61
10	DNRA	$2CH_2O + NO_3^- + H^+ \rightarrow NH_4^+ + HCO_3^- + CO_2$	C $\rightarrow$ N: 8	0.58
11	Anammox	$NH_4^+ + NO_2^- \rightarrow N_2 + 2H_2O$	N $\rightarrow$ N: 3	1.00
12	Heterotrophic Mn(IV) reduction	$CH_2O + 2MnO_{2(s)} + 3H^+ \rightarrow 2Mn^{2+} + HCO_3^- + 2H_2O$	C $\rightarrow$ Mn: 2	9.15
13	Heterotrophic Fe(III) reduction	$CH_2O + 4Fe(OH)_{3(s)} + 7H^+ \rightarrow 4Fe^{2+} + HCO_3^- + 10H_2O$	C $\rightarrow$ Fe: 1	18.60
14	Fe(III) reduction	$9HS^- + 8Fe(OH)_{3(s)} + 7H^+ \rightarrow 8FeS_{(s)} + SO_4^{2-} + 20H_2O$	S $\rightarrow$ Fe: 1	1.50
15	Fe(III) reduction	$3HS^- + 2FeOOH_{(s)} \rightarrow 2FeS_{(s)} + S_{(s)} + H_2O + 3OH^-$	S $\rightarrow$ Fe: 1	1.13
16	Heterotrophic SO$_4^{2-}$ reduction	$2CH_2O + SO_4^{2-} \rightarrow HS^- + 2HCO_3^- + H^+$	C $\rightarrow$ S: 8	4.00
17	SO$_4^{2-}$ reduction	$9Fe^{2+} + SO_4^{2-} + 20H_2O \rightarrow FeS_{(s)} + 8Fe(OH)_{3(s)} + 16H^+$	Fe $\rightarrow$ S: 7	0.19
18	S^{2-} oxidation	$FeS_{(s)} + H_2S \rightarrow FeS_{2(s)} + H_2$	S $\rightarrow$ H: 1	0.61
19	Methanogenesis	$4H_2 + CO_2 \rightarrow CH_4 + 2H_2O$	H$_2$ $\rightarrow$ C: 8	5.46

change, which was then used to compute an adjusted SO_4^{2-} concentration. The one-third factor was applied to reflect differences in Cl$^-$ and SO_4^{2-} retardation factors reported by Pachepsky et al. (1994), who indicated SO_4^{2-} retardation factors about three times those of Cl$^-$ for a clay soil not unlike those beneath the stormwater basin. The prevalence of kaolinite (as high as 48% of the clay fraction; W.G. Harris, personal communication, 2009) and Fe and Al oxides (Fig. 3B, C) suggest the potential for anion sorption. Therefore, the adjusted SO_4^{2-} concentrations provide an estimate of what concentrations would have been in the absence of the physicochemical processes inferred from the Cl$^-$ variations (Supplemental Fig. S2 and S3).

Similar Cl$^-$ concentrations in groundwater from well PW and in stormwater, compared to large differences in concentrations of N and C species as well as DO, Mn, Fe and SO_4^{2-} (Figs. 4 and 5), suggest a reaction dominated fate of these redox sensitive constituents that is related to subsurface biogeochemical processes. These results are interpreted in the following sections in the context of the redox reactions in Table 1 in order to better understand the biogeochemical processes beneath the basin.

3.5. Biogeochemical processes

Water chemistry changes resulting from redox reactions are usually mediated by subsurface microorganisms as they use the energy produced during electron transfer for growth. Due to its relative prevalence in the subsurface, OC commonly serves as an electron donor coupled to the following sequence of electron acceptors, $O_2 > NO_3^- > Mn(IV) > Fe(III) > SO_4^{2-}$

CO_2, referred to as the ecological succession of terminal electron-accepting processes (TEAPs) (Chapelle et al., 1995; McMahon and Chapelle, 2007).

Biogeochemical processes in groundwater beneath the basin were inferred from cyclic variations in the chemistry of the following redox reactants and products: DOC (reactant), DO (reactant), NO_3^- (reactant), Mn^{2+} (product), Fe^{2+} (product), SO_4^{2-} (reactant; using the adjusted values shown in Supplemental Fig. S3) and alkalinity (product) (Fig. 5). All of the TEAPs were identified beneath the stormwater basin. Redox reactant concentrations were depleted or product concentrations increased in a time sequence according to the thermodynamically-governed order of TEAPs. To gain further insight into these biogeochemical processes, electron equivalents were computed based on millimolar concentrations and the number of electrons transferred during the redox reaction (Postma et al., 1991). DOC with zero valent C was assumed to be the only electron donor, with complete oxidation to CO_2 (4 electrons transferred), using CH_2O as a simplified representation of organic matter. Dissolved inorganic carbon (DIC) was computed as the sum of CO_2 and alkalinity (HCO$_3^-$) (Fig. 7A); when dissolved gas samples were not collected, CO_2 was estimated based on linear regression between alkalinity and CO_2 ($r^2 = 0.59$, $n = 7$). The following number of electrons are transferred in each TEAP (see Table 1 for the stoichiometric reaction referenced by the equation number): O_2 (4 electrons, equation 5), NO_3^- (5 electrons, equation 6), Mn(IV) (2 electrons, equation 12), Fe(III) (1 electron, equation 13) and SO_4^{2-} (8 electrons, equation 16). The cyclic variations in groundwater chemistry (Fig. 5) and in electrons transferred (Fig. 7B) are presented
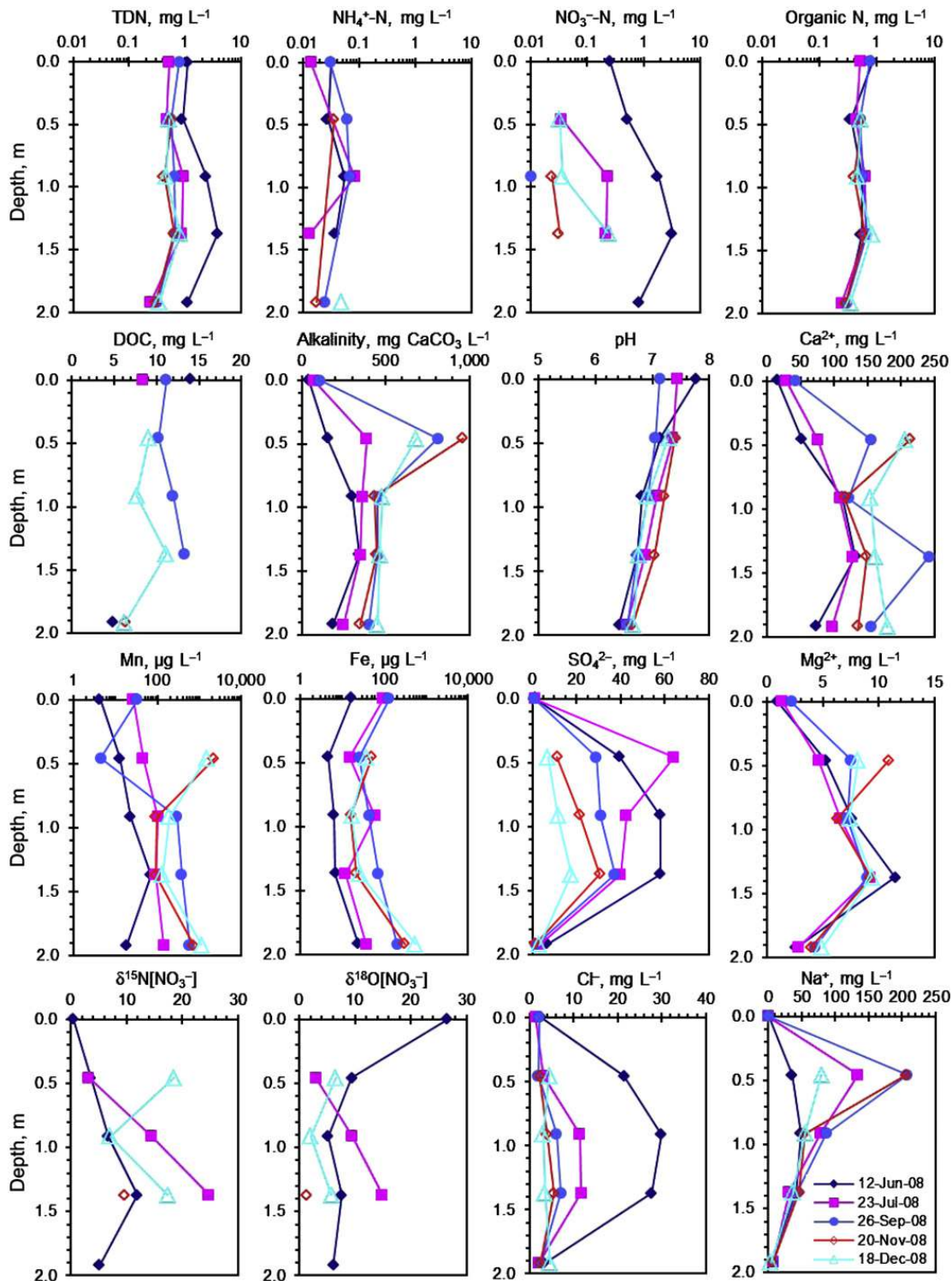
Fig. 6. Soil–water and groundwater chemistry profiles beneath the stormwater infiltration basin. Data at 0-m depth represent stormwater samples; data at 0.5, 0.9 and 1.4-m depths represent lysimeter samples; data at 1.9-m depth represent well PW. Data is not available at every depth for every sampling event due to lack of sample (stormwater), lack of analysis for that sample (dissolved organic carbon, DOC; $\delta^{15}N[NO_3^-]$; $\delta^{18}O[NO_3^-]$), or non-exceedance of detection limit ($NH_4^+–N$, $NO_3^-–N$). $NO_2^-–N$ was typically below the laboratory reporting limit of 0.002 mg L^{-1} for all soil–water and groundwater samples, with the exception of June and July samples at 0.5 and 0.9 m depths where $NO_2^-–N$ ranged from 0.0027 to 0.0072 mg L^{-1}. Organic N is computed as the difference between total dissolved nitrogen (TDN) and inorganic nitrogen ($IN = NH_4^+ + NO_3^- + NO_2^-$), where NH_4^+, NO_3^- and NO_2^- are assumed zero when below their respective method detection limits of 0.01, 0.008 and 0.001 mg L^{-1}.

in the following sections as evidence for each biogeochemical process, followed by a discussion of the time scales of variations and impacts on N fate.

3.5.1. Organic carbon oxidation

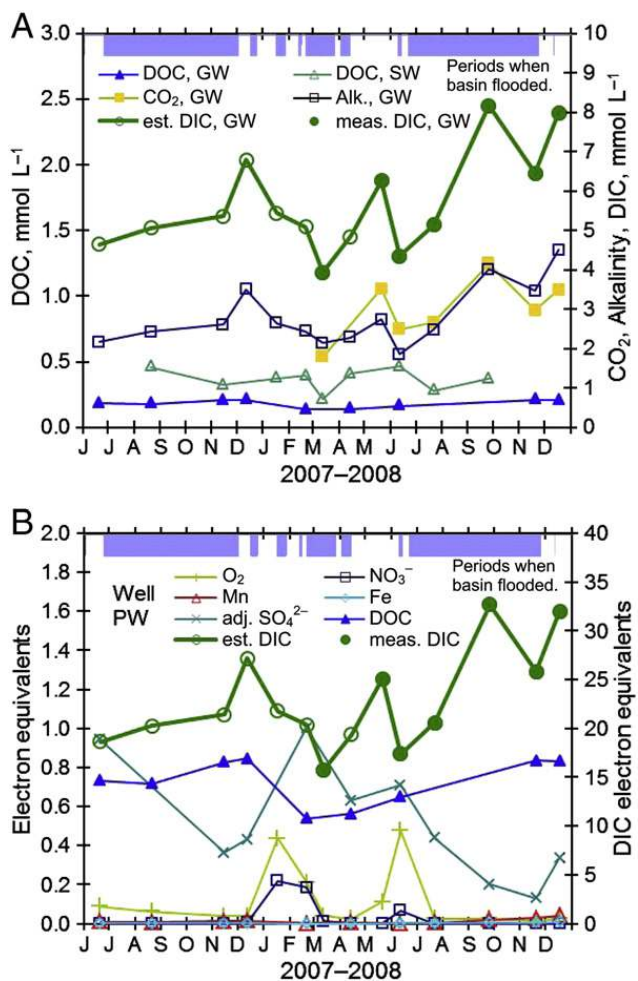Organic matter oxidation during TEAPs results in decreases in DOC concentrations and increases in CO_2 and

Fig. 7. Select reactants or products participating in heterotrophic terminal electron accepting processes observed in groundwater beneath the storm-water infiltration basin (well PW) (A) molar concentrations of organic and inorganic carbon species; and (B) electron equivalents for select reactants or products of each terminal electron accepting process. Alk, alkalinity; DIC, dissolved inorganic carbon where "est." denotes estimated values and "meas." denotes measured values; DOC, dissolved organic carbon; GW, groundwater samples; SW, stormwater samples; adj. SO_4^{2-}, sulfate data adjusted based on comparison to chloride concentrations.
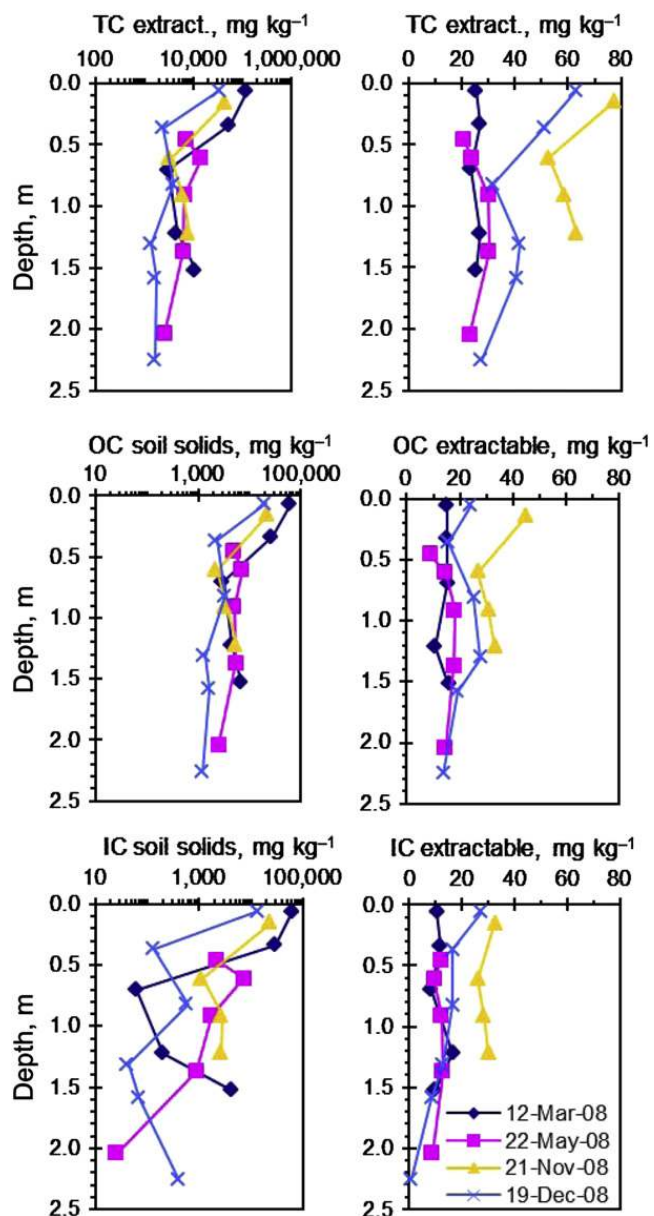

Fig. 8. Soil solid and water extractable total carbon (TC), organic carbon (OC) and inorganic carbon (IC) contents beneath the stormwater infiltration basin. IC is computed as the difference between TC and OC.

HCO_3^- concentrations (DIC). However, other physical or geochemical processes can affect these concentrations, such as source inputs (infiltration of stormwater), solid/aqueous phase interactions, and gas/aqueous phase interactions. Groundwater DOC tended to increase during prolonged flooding of the basin in 2007 and 2008 (Fig. 5B), possibly due to infiltration of stormwater with DOC concentrations about twice that of groundwater (Fig. 4B). During the intervening period of intermittent or no flooding (winter and spring in 2008), groundwater DOC decreased, possibly due to oxidation or reduced stormwater infiltration.

Variations in OC and IC concentrations in soil and water samples suggest biogeochemical activity. Groundwater DIC generally increased during prolonged flooding of the basin in 2007 and 2008 (Fig. 7A), which could be due to both carbonate mineral dissolution and oxidation of DOC. Carbonates in soil sediments are the probable source of soil solid IC contents typically exceeding 1000 mg kg^{-1} (0.1%) (Fig. 8). Results of soil water extractable analyses generally indicate increases in water extractable OC and IC concentrations

from spring (March and May samples) to autumn (November and December samples) in 2008 at depths less than 1.3 m, but were generally unchanged below this depth (Fig. 8). The increases in water extractable OC may be caused by mass transfer of OC between solid and aqueous phases, although soil solid OC contents are so large that such changes are not discernible, or OC input from infiltrating stormwater. Increases in water extractable IC from spring to autumn 2008 may be indicative of a zone of active biogeochemical processes in the shallow soil zone 0–1.3 m deep. Increases in alkalinity for the lysimeter samples also indicate increases in soil water and groundwater HCO_3^- at depths above 1.4 m at the prevailing pH values 6.5–7.5 (Fig. 6). Substantial changes in soil solid IC at values less than 1000 mg kg^{-1} probably are largely the result of analytical variability because IC is computed as the difference between measured TC and OC. DIC increases exceed 10 times the number of electrons transferred

during all TEAPs (Fig. 7B) and elevated Ca^{2+} concentrations (Fig. 6) yield calcite saturation indices greater than 1.5 in the zone of high alkalinity (0.5–1.4 m depths), further indicating that DIC variations are dominated by carbonate chemistry. However, similar temporal variations in CO_2 and HCO_3^- (alkalinity) with a general upward trend (Fig. 7A) while pH was also increasing (Fig. 5C) are suggestive of DOC use as a reductant for the TEAPs, thus part of the increase in groundwater DIC is likely caused by DOC oxidation and can account for the electrons transferred in all TEAPs (Fig. 7B).

To identify whether sufficient electrons are available from stormwater DOC to supply the total transferred during the observed TEAPs, an electron balance for heterotrophic processes in the upper soil zone was developed. The soil zone examined spanned from the bottom of the basin to 1.9 m deep (the midpoint of the screened interval of well PW). The 162-d period from 11 June to 20 November 2008 was selected as this represented the period of generally prolonged flooding of the basin during which a sequence of TEAPs was observed. Hydrologic monitoring indicates that this is a typical seasonal flooding pattern for this stormwater basin, thus results may be representative of behavior during other years (Fig. 2B). The electron balance was developed by (1) assuming one-dimensional steady downward flow through a control volume with a 1 m^2 cross-sectional area; (2) using an infiltration rate of 20 mm d^{-1} and porosity of 0.40; (3) using the analyte concentrations in stormwater for inflow to the control volume and in well PW for outflow from the control volume; and (4) estimating the changes in electron storage within the control volume by integration of analyte concentrations over the 1.9-m depth using data from stormwater, lysimeter (0.5, 0.9 and 1.4 m depths) and well PW samples.

The large decrease in DOC between stormwater and well PW is equal to a loss of about 6020 electron equivalents, representing a net addition of electrons to the control volume. Heterotrophic TEAPs occurring within the control volume represent a net "electron demand," and may consist of O_2, NO_3^-, Mn(IV), Fe(III) and SO_4^{2-} reduction. SO_4^{2-} reduction accounts for most of the electrons accepted, about 910 electron equivalents. DO measurements were only available for stormwater and well PW, thus the electrons transferred in the control volume by O_2 reduction can be estimated only very coarsely at about 380 electron equivalents. NO_3^- reduction accounts for about 100 electron equivalents. Mn and Fe reduction represent a small net gain of about 20 electron equivalents due to the increase in concentrations over this period, although more electrons may have been transferred that were not reflected in aqueous concentrations if Mn^{2+} and Fe^{2+} are consumed in other reactions (for example, equations 7, 8, 9 and 17 in Table 1). The net quantity of electron equivalents transferred in the control volume, or the electron demand, was about 1370 and represents 4650 less than what was supplied by infiltrating stormwater assuming that all of the decrease in DOC represents a labile fraction and was oxidized. This discrepancy may be attributable to one or more of the following factors: (1) stormwater DOC is of relatively young humic origin due to the frequent submergence and subsequent decomposition of herbaceous vegetation during flooding, and thus was relatively labile because organic matter reactivity typically is inversely correlated with age (Appelo and Postma, 2005); (2) some of the labile fraction

of the infiltrating DOC was involved in other reactions such as complexation or sorption; (3) sparse temporal resolution of DOC data (only three samples of stormwater and two for well PW) introduced error into the computed net DOC decrease; and (4) greater spatial variability occurred in TEAPs than could be resolved by the 0.5-m sampling-depth intervals. Nevertheless, soil water extractable OC contents generally exceeding 10 mg kg^{-1} and soil solid OC generally exceeding 1000 mg kg^{-1} (Fig. 8) are considerably larger than the estimated electron demand, which is equivalent to a soil OC content of only 3.5 mg kg^{-1}. Thus, between DOC in infiltrating stormwater and solid phase OC, sufficient labile OC likely exists to permit heterotrophic metabolism for all observed biogeochemical processes.

3.5.2. Oxygen reduction

DO in groundwater beneath the basin was always substantially lower than that in stormwater (Figs. 4A and 5A). Groundwater DO was quickly depleted as flooding continued, and was less than or equal to 0.5 mg L^{-1} for 9 of the 14 sampling events. The lowest groundwater DO concentration of 0.1 mg L^{-1} occurred in November 2008, toward the end of the prolonged flooding when the stormwater DO was also unusually low. O_2 reduction likely was coupled with DOC oxidation (equation 5, Table 1), as ample DOC was available to account for the required electron transfer (Fig. 7B). The ensuing anoxic conditions enabled the progression of TEAPs.

3.5.3. Nitrate reduction

Concomitant peaks in groundwater DO and NO_3^- concentrations occurred beneath the basin (Fig. 5A), whereas stormwater TDN was consistently composed primarily of ON (Fig. 4A), indicating short periods of ammonification/nitrification. For example, elevated groundwater TDN concentrations exceeded 1 mg L^{-1} (primarily in the NO_3^- form) for the 12 June 2008 sample (Fig. 6) and was caused by infiltration of oxygenated stormwater from a rainfall event about two days prior to collection of the sample. However, similar to DO, NO_3^- in groundwater was short lived and was depleted below 0.1 mg L^{-1} for 65% of the samples collected from well PW (Fig. 5A) and the lysimeters (Fig. 6). Samples from the lysimeters were only collected during the summer and autumn of 2008 (before, during and after the prolonged flooding). TDN in groundwater and soil water was predominantly in the form of ON, whereas NH_4^+–N was less than 0.1 mg L^{-1} (Figs. 5A and 6). NO_3^- reduction likely was coupled with DOC oxidation (Fig. 7B).

Soil N chemistry differed in the spring (March and May 2008) before the summer wet period compared to autumn (November and December 2008) after the prolonged flooding. The near absence of NO_3^- in water extractable samples in autumn is suggestive of denitrification (equation 6, Table 1) or dissimilatory nitrate reduction to ammonium (DNRA) (equation 10, Table 1) during the summer wet season (Fig. 9). Soil water extractable NO_2^- was low and typically less than 10% of NO_3^- (Fig. 9). The slightly increased NH_4^+ concentrations in November may be due to DNRA, whereas the decreased NH_4^+ combined with low NO_3^- concentration in December probably is due to nitrification (equations 4a and 4b, Table 1) in the uppermost soil layers as the basin dried and NO_3^- reduction in the portions of the underlying
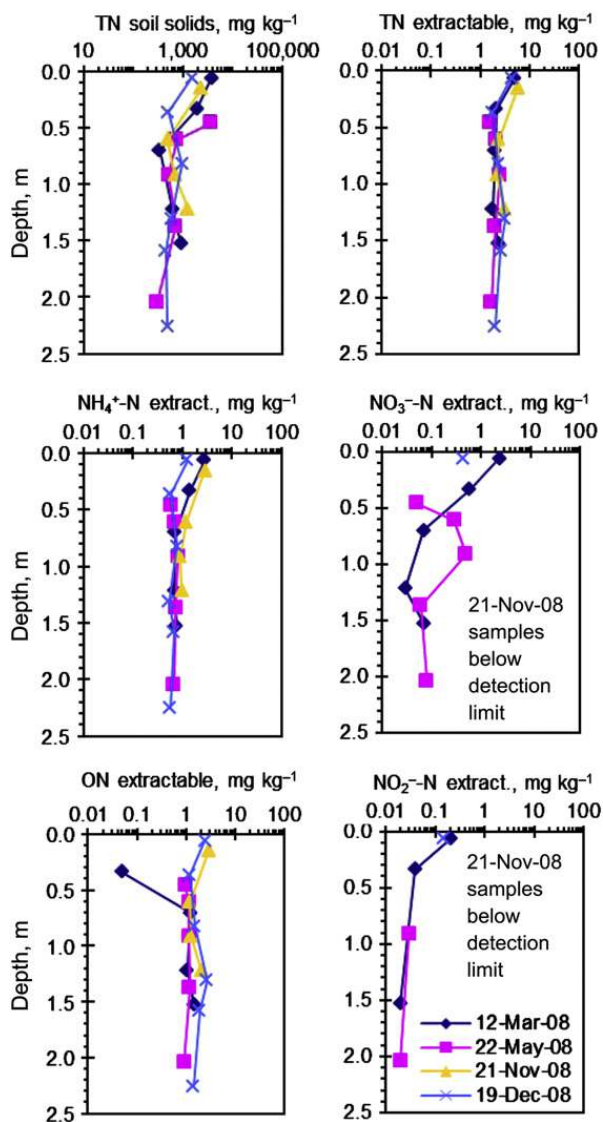
Fig. 9. Soil solid and water extractable total nitrogen (TN) and soil water extractable ammonium nitrogen (NH_4^+), nitrate (NO_3^-), nitrite (NO_2^-) and organic nitrogen (ON) beneath the stormwater infiltration basin. Organic N is computed as the difference between total nitrogen (TN) and inorganic nitrogen ($IN = NH_4^+ + NO_3^- + NO_2^-$), where NO_3^- and NO_2^- are assumed zero when below the method detection limit. Data are not available at every depth for every sampling event due to negative computed ON or non-exceedance of NO_3^- and NO_2^- detection limit.
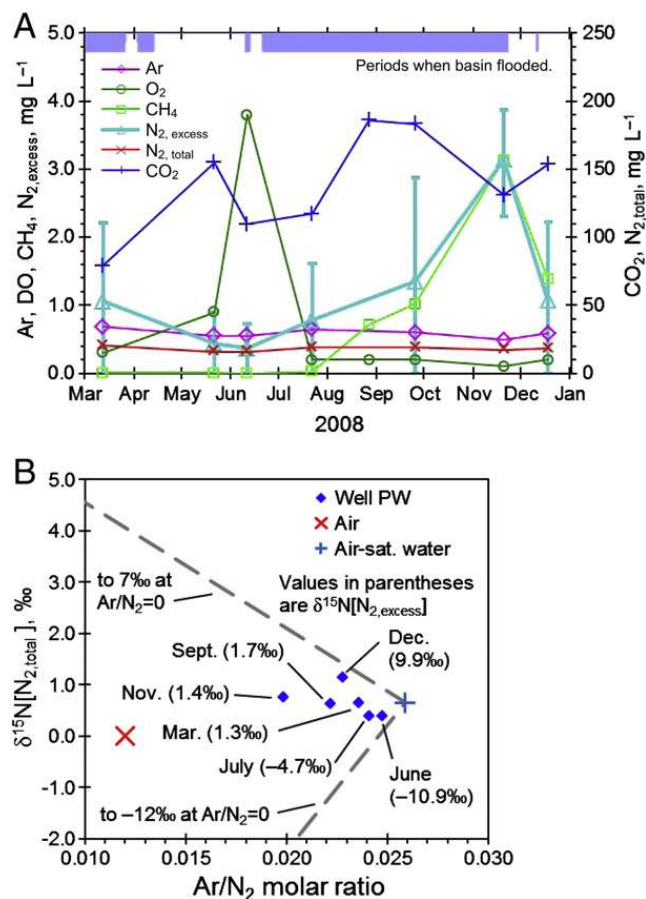

Fig. 10. Dissolved gas concentrations in groundwater beneath the stormwater infiltration basin: (A) temporal variations in dissolved gasses and excess N_2 (error bars for excess N_2 indicate the range of reasonable values given uncertainty in recharge temperatures); and (B) $\delta^{15}N$ of N_2 and Ar/N_2 ratios. All samples were collected in 2008 from well PW, except the August sample which was collected from well M-0512. CO_2, CH_4 and O_2 concentrations are expected to be comparable at these two wells at this time due to extensive flooding of the basin (2.0 m deep at PW and 1.0 m deep at M-0512) and similar well depths (mid-screen depths of 1.9 m for PW and 1.7 m for M-0512).

soil zone that remained saturated (Fig. 9). The presence of NH_4^+ and NO_2^- in soil water extracts (Fig. 9) could indicate the possibility of anaerobic ammonium oxidation (anammox, equation 11, Table 1) contributing to NO_3^- reduction (Clark et al., 2008), although data are insufficient to confirm whether anammox was or was not occurring. In order to investigate N cycling in greater detail and better determine the predominant NO_3^- reduction pathway, denitrification or DNRA, dissolved gasses and stable isotopes were examined.

3.5.3.1. Dissolved gasses. DO was measured in the field during each sample event, but additional dissolved gas samples (Ar, N_2, CO_2, CH_4) were collected during spring, summer and autumn 2008 to better understand biogeochemical activity and its seasonal variation, particularly for denitrification (Fig. 10A). N_2 and other atmospheric and biogenic gasses

can be present in the saturated zone in aqueous form or as gas phase bubbles (Vogel et al., 1981). Analysis of dissolved gas concentrations, particularly N_2 and Ar, in the groundwater beneath the stormwater infiltration basin permits estimation of the amount of excess air and excess N_2. Excess air is the dissolved atmospheric gas in excess of that attributable to atmospheric equilibration of the water during infiltration and transport through the unsaturated zone (Aeschbach-Hertig et al., 2008). Excess N_2 is the fraction of dissolved N_2 in excess of that attributable to atmospheric solubility equilibrium and is commonly attributed to denitrification, but also can be produced by anammox (equations 6–9 and 11, Table 1).

Excess N_2 was computed using the measured concentrations and computed solubilities of N_2 and Ar (Weiss, 1970), atmospheric pressure, and recharge temperature based on the methodology described by Green et al. (2008b). Recharge temperature is the temperature of the recharge water, infiltrated stormwater in this case, at that point in the flow process where the water is no longer able to equilibrate with atmospheric gasses, commonly estimated to be at the depth

of the top of the capillary fringe or water table. Due to the dynamic nature of the groundwater system beneath a stormwater infiltration basin, there is considerable uncertainty in determining the exact timing of the infiltration event (and hence tracking the corresponding recharge temperature). The method is sensitive to recharge temperature, but reliable recharge temperatures could not be independently estimated at this site. As an alternative, minimum (excess $N_2 = 0$) and maximum (excess air = 0) values of excess N_2 were assumed and the corresponding recharge temperatures were estimated iteratively to meet each criterion. The final estimated recharge temperature was computed as the average of the estimated minimum (for excess air = 0 criterion) and maximum (for excess $N_2 = 0$ criterion) recharge temperatures. To further constrain results, the average recharge temperature was compared to measured subsurface temperatures. A 7-d moving window average was computed for temperature at 0.3 m depth (Fig. 2C), resulting in a range of realistic recharge temperatures of 12.6–29.2 °C. Only for the 20 November 2008 sample (average estimated recharge temperature = 33.6 °C) was it necessary to adjust the recharge temperature, which was set equal to the 0.3 m subsurface temperature of 28.7 °C on 10 June 2008, the date of the first major infiltration event of the summer wet season. This infiltration event substantially reduced the thickness of the unsaturated zone (water table rose from a depth of 2.5 m on 9 June to a depth of 0.4 m on 11 June; Fig. 2B), which became fully saturated during the prolonged flooding period beginning 21 June 2008, and thus contributed to the anoxic groundwater conditions favorable for NO_3^- reduction (Fig. 5A). The excess N_2 measured in the 20 November 2008 sample may have resulted from reduction of elevated NO_3^- concentrations in recharge that occurred during this infiltration event (see 12-Jun-08 sample, Fig. 6) in the biogeochemically active zone (0–1.4 m depth) inferred from C cycling discussed in Section 3.5.1.

Excess N_2 was present in groundwater beneath the basin from well PW for all samples, ranging from 0.4 to 3 mg L^{-1} (Fig. 10A), suggesting that denitrification affected these samples. However, it should be noted that due to the uncertainty in recharge temperatures, only the 20 November 2008, sample had a minimum excess N_2 greater than zero (2.3 mg L^{-1}). Nevertheless, the temporal pattern of the estimated excess N_2 concentrations is in agreement with other redox conditions, being low when O_2 and NO_3^- were elevated and high under anoxic conditions. For the May and June samples, the estimated maximum excess N_2 concentrations were less than 1 mg L^{-1} and DO was 0.9 and 3.8 mg L^{-1}, respectively. Such low values for estimated maximum excess N_2 concentrations might be interpreted as essentially zero given the data presented by Green et al. (2008b), which show that 95% of strictly aerobic samples (DO exceeding 1.6 mg L^{-1}) had excess N_2 less than 1.3 mg L^{-1} (0.047 mmol L^{-1}). Higher excess N_2 concentrations were most likely present in March, July, September, November and December, when the range of estimated values (indicated by the error bars in Fig. 10A) plots at least partially above 1 mg L^{-1}, providing supporting evidence for denitrification during or prior to these times. For the March sample, the low NO_3^-–N concentration (0.17 mg L^{-1}) possibly represented residual NO_3^- that had not been denitrified (Fig. 5A). In contrast, NO_3^-–N

concentrations were below the laboratory method detection limit (0.008 mg L^{-1}) for the July through December samples (Fig. 5A). N_2 can also be produced by anammox (equation 11, Table 1). Consistently low NH_4^+ and NO_2^- concentrations in soil water and groundwater (Figs. 5A and 6) suggest limited significant excess N_2 attributable to anammox. However, soil water extractable NH_4^+ and NO_2^- concentrations (NO_2^-–N of 0.15 mg kg^{-1} for 19 December 2008 (Fig. 9), equivalent to 0.47 mg L^{-1}) could yield 0.47 mg L^{-1} excess N_2 (equation 11, Table 1). These data suggest that anammox cannot be definitively precluded as a potentially important pathway for N cycling in the subsurface.

3.5.3.2. Stable isotopes of nitrogen and oxygen. Results of the N and O isotopic analysis of NO_3^- for stormwater, soil water and groundwater samples provide insight into the sources of NO_3^- and differences in NO_3^- biogeochemistry at the study site (Fig. 11A). The precipitation samples were collected at a nearby stormwater infiltration basin (Hunter's Trace, Fig. 1) and, as expected, indicate an atmospheric source of NO_3^-. The stormwater sample is indicative of atmospheric or fertilizer-derived NO_3^-. Many groundwater samples and the one soil–water sample are indicative of nitrification of one or more of the following: atmospheric or fertilizer-derived NH_4^+, soil nitrogen (organic or NH_4^+), or organic waste (manure or septic). N contamination from organic waste sources is believed to be limited. The watershed drains a residential area with no large-scale agricultural pollution (manure). Residences within the watershed and immediately surrounding the stormwater infiltration basin (Fig. 1) are served by septic tanks. Septic tank leachate possibly could impact groundwater at the wells sampled at the stormwater infiltration basin, however hydraulic gradients and travel times indicate that this potential is limited. Median water-table gradients were small, indicating a groundwater travel time from nearby septic tanks of at least 20 years, and vertical groundwater gradients were always downward and at least an order of magnitude larger than water-table gradients, which suggests that drainage from septic tanks would not intercept the monitoring zone of the shallow wells. Given the residential surroundings, animal (pet) waste is another potential source of organic N, but $\delta^{15}N[NO_3^-]$ values between this site and the nearby Hunter's Trace site (Fig. 1) are substantially different (Wanielista et al., 2011), even though pet waste contributions probably are similar between sites. Therefore, the source of NO_3^- likely is fertilizer-impacted stormwater runoff and nitrification of soil N rather than groundwater movement from adjacent areas, and enriched isotope ratios are more indicative of denitrification than an organic source.

Further evidence of nitrification is given by a comparison of $\delta^{18}O[NO_3^-]$ and $\delta^{18}O[H_2O]$. Research has indicated that nitrification derives oxygen from water molecules and O_2 in a predictable manner according to the two-step microbially mediated reactions: (1) NH_4^+ oxidation to NO_2^- by *Nitrosomonas* uses one oxygen from water and one from O_2 (equation 4a, Table 1); and (2) NO_2^- oxidation to NO_3^- by *Nitrobacter* uses one oxygen from water (equation 4b, Table 1) (Kendall, 1998). If the process occurs without fractionation, the $\delta^{18}O[NO_3^-]$ can be computed simply as 2/3 $\delta^{18}O[H_2O] + 1/3 \delta^{18}O[O_2]$ and assuming a $\delta^{18}O[O_2]$ of 23‰ characteristic of atmospheric O_2 (Kendall, 1998). Several
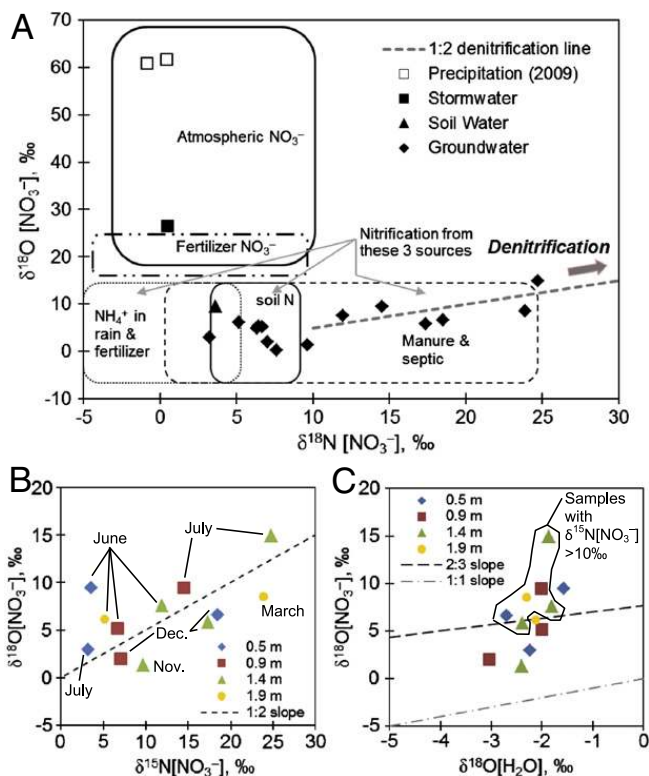
Fig. 11. Isotope ratios for (A) $\delta^{15}N$ and $\delta^{18}O$ of NO_3^- in precipitation, stormwater, soil water, and groundwater plotted relative to typical source ranges from Kendall (1998); (B) $\delta^{15}N$ and $\delta^{18}O$ of NO_3^- in soil water and groundwater; and (C) $\delta^{18}O$ of NO_3^- and $\delta^{18}O$ of H_2O in soil water and groundwater. All samples were collected at the South Oak site in 2008 with the exception of precipitation samples collected at the Hunter's Trace site in May and December 2009 (Fig. 1).

groundwater samples plot near the 2:3 slope line of $\delta^{18}O$ [NO_3^-] and $\delta^{18}O[H_2O]$, and several plot between this line and the 1:1 slope line that represents the trend if all oxygen during nitrification was derived from H_2O (Fig. 11C). These results suggest that nitrification occurred at times beneath the basin. Green et al. (2008b) report data that fall closely along the 2:3 slope line from several agricultural areas across the United States where the groundwater was aerobic ($O_2 > 0.5$ mg L^{-1}) and they noted other evidence indicating nitrification was occurring. Katz et al. (2010) report data from soil water and groundwater samples collected in septic tank drain fields in northwest Florida with a relatively large range of $\delta^{18}O[NO_3^-]$ and with nearly all samples falling between the 1:1 and 2:3 slope lines; nonetheless, denitrification was identified as one of the likely mechanisms for NO_3^- loss in the drain fields. For the samples collected from groundwater beneath the stormwater basin, considerably greater variability existed in $\delta^{18}O[NO_3^-]$ compared to $\delta^{18}O$ [H_2O] and several samples fall well above the 2:3 slope line (Fig. 11C). Values that plot above the 2:3 slope line indicate that either enriched $\delta^{18}O[O_2]$ was being used for nitrification (values of $\delta^{18}O[O_2]$ of soil air can be as high as 60‰ because of respiration derived fractionation (Kendall, 1998)) or $\delta^{18}O$ [NO_3^-] had been fractionated by denitrification. In the latter case, comparison of $\delta^{18}O[NO_3^-]$ and $\delta^{15}N[NO_3^-]$ can provide evidence of denitrification.

Enriched values of $\delta^{15}N[NO_3^-]$, and to a lesser degree of $\delta^{18}O[NO_3^-]$, occur during bacteriological denitrification with a ratio of $\delta^{18}O{:}\delta^{15}N$ of about 1:2 (Kendall, 1998; Kendall and Aravena, 2000). Six groundwater samples from this study fell closely along this line and are more highly enriched

($\delta^{15}N[NO_3^-] > 10‰$) relative to the other groundwater samples; these samples are consistent with the effects of denitrification (Fig. 11A). Other samples with $\delta^{15}N[NO_3^-]$ less than 10‰ also follow this 1:2 slope line (Fig. 11B). One exception is the sample at a 0.5-m depth collected 12 June 2008, after a runoff event 10 June. Water-table depth on 12 June 2008 was 0.55 m, increased from 2.5 m deep on 9 June, and thus represents very recent infiltration in the relatively aerobic unsaturated zone (moisture contents increased from 76 to 86% saturation) (Fig. 2B, C). Recharge from this infiltrating stormwater (the stormwater sample shown in Fig. 11A was collected on 12 June) sampled in the 0.5-m deep lysimeter falls well above the 1:2 slope line (Fig. 11B), and this sample is more indicative of nitrification as suggested by $\delta^{18}O[NO_3^-]$ and $\delta^{18}O[H_2O]$ values if enriched $\delta^{18}O[O_2]$ was being used for nitrification (Fig. 11C). In contrast, lysimeter samples from below the water table (1.4 and 1.9 m depths) on this date indicate enriched $\delta^{15}N[NO_3^-]$ and $\delta^{18}O[NO_3^-]$ with depth (Fig. 6), following the 1:2 slope line indicating denitrification (Fig. 11B). Additionally, lysimeter samples for 23 July 2008, after the basin had been flooded 32 days, indicate progressively enriched $\delta^{15}N[NO_3^-]$ and $\delta^{18}O[NO_3^-]$ with depth (Fig. 6), following the 1:2 slope line indicating denitrification (Fig. 11B). These results are consistent with the zone of organic matter oxidation at depths above 1.4 m as suggested by OC and IC concentrations from soil water extracts (Fig. 8) and from lysimeters (Fig. 6), which was discussed in Section 3.5.1.

Comparison of excess N_2 and isotopic fractions is possible for only the 12 March and 12 June 2008 samples from well PW, when NO_3^-–N concentrations were above the minimum

value required for isotopic analysis (0.03 mg L^{-1}) (Fig. 5A). For the March sample, collected 29 d after flooding of the basin, isotopic enrichment was evident (δ^{15}N[NO$_3^-$] of 24‰ and δ^{18}O[NO$_3^-$] of 8.5‰, Fig. 11B) and excess N$_2$ was 1 mg L^{-1} (Fig. 10A), suggesting that denitrification had depleted much of the initial NO$_3^-$. Whereas nitrification was indicated for the June sample (δ^{15}N[NO$_3^-$] of 5.2‰ and δ^{18}O [NO$_3^-$] of 6.1‰, Fig. 11B), which was collected 27 h after a 26-mm storm event resulting in temporary storage of stormwater up to 0.28 m deep, where a high DO and an elevated NO$_3^-$–N concentration of 0.84 mg L^{-1} was measured. If this rapid change in groundwater quality in well PW (mid-screen depth of 1.9 m) is assumed to be attributable to this single infiltration event, which is reasonable given that no appreciable rainfall had occurred since early April (Fig. 2A), infiltrated stormwater was percolating at a rate of at least 1.7 m d^{-1}. When compared with a saturated Darcian pore-water velocity of 0.045 m d^{-1}, these results suggest a preferential flow system with rapid flow through macropores and slower flow through the soil matrix. Given that the soil was not fully saturated prior to this runoff event, the unsaturated Darcian pore-water velocity would be considerably lower and is estimated to be 0.001 m d^{-1} at a 0.6-m depth (based on soil properties reported by Naujock, 2008, measured volumetric moisture content, and an assumed hydraulic gradient of 1 m m^{-1}). The rapid percolation caused by macropores likely delivered initial recharge to greater depths by largely bypassing the 0–1.4 m biogeochemically active zone, resulting in reduced opportunity for denitrification. An excess N$_2$ concentration in June of essentially zero (Fig. 10A) and lower δ^{15}N[NO$_3^-$] at a depth of 1.9 m compared to shallower depths (0.9 and 1.4 m, Fig. 11B) are consistent with this conceptual model. These results suggest that the assumption of Darcian flow in such a soil is inaccurate for solute transport analyses, and is consistent with those of Kurtzman and Scanlon (2011) who describe the importance of preferential flow paths for explaining observed Cl$^-$ concentrations in an expansive clay soil.

Additional insight on potential denitrification can be gleaned from δ^{15}N[N$_2$] values for groundwater samples collected from well PW because excess N$_2$ will be depleted in δ^{15}N relative to the NO$_3^-$ from which it was formed. The δ^{15}N value of the total measured dissolved N$_2$ is denoted as δ^{15}N[N$_{2,total}$], whereas the δ^{15}N value of excess N$_2$ is denoted as δ^{15}N[N$_{2,excess}$] and is derived by linear mixing calculation using δ^{15}N of air-saturated water of 0.7‰ (Böhlke et al., 2002; Green et al., 2008b). Data are shown on Fig. 10B relative to dashed mixing lines drawn between atmospheric (Ar/N$_2$ molar ratio of 0.0259) and non-atmospheric (Ar/N$_2$ molar ratio of 0.0) excess N$_2$ for representative samples where denitrification was relatively incomplete (lower mixing line, δ^{15}N[N$_{2,excess}$] = −12‰) and relatively complete (upper mixing line, δ^{15}N[N$_{2,excess}$] = 7‰) in a fashion analogous to that presented by Böhlke et al. (2002). When denitrification is complete, the δ^{15}N[N$_{2,excess}$] should equal δ^{15}N [NO$_3^-$] of the source (Böhlke et al., 2002). Nitrification of soil N is a likely source of NO$_3^-$ beneath the basin as described previously, and 7‰ approximates the δ^{15}N[NO$_3^-$] of many of these samples (Fig. 11A). Results suggest that the samples collected from well PW represent the effects of denitrification reactions in various stages of completion. δ^{15}N[N$_{2,excess}$]

increased from −10.9‰ in June 2008 to 9.9‰ in December 2008, with samples from the beginning of the prolonged flooding period (June and July) plotting nearest to the mixing line representing relatively incomplete denitrification and the sample from December plotting nearest to the mixing line representing relatively complete denitrification (Fig. 10B). It is important to note that δ^{15}N[N$_2$] variations also can result from variations in the isotopic composition of the NO$_3^-$ source and mixing of denitrified and undenitrified water (Böhlke et al., 2002), as well as other NO$_3^-$ reduction pathways such as DNRA or anammox (Böhlke et al., 2006). Nevertheless, δ^{15}N[N$_2$] values are consistent with other stable isotope (Fig. 11) and dissolved gas (Fig. 10A) results, all of which are consistent with denitrification.

3.5.4. Manganese and iron reduction

Anoxic conditions in the subsurface enabled the loss of NO$_3^-$ as well as leading to increases in Mn and Fe in groundwater (Fig. 5C), which probably are due to bacterially-mediated processes (equations 12 and 13, Table 1) and the greater solubility of reduced Mn and Fe (Appelo and Postma, 2005). Presumably, the Mn and Fe concentrations consist of the reduced valence states of Mn^{2+} and Fe^{2+}. Soil chemical analyses indicate Fe oxide contents as high as 20,000 mg kg^{-1} that can serve as the source of Fe^{3+} (Fig. 3B), and Mn oxides are often associated with Fe oxides in subsurface sediments (Schulze, 2002). Solid phase Fe oxides are likely reactive, based on the prevalence of amorphous Fe oxides from acid-ammonium-oxalate (AAO) extractions about equal to or exceeding citrate-dithionite-bicarbonate (CDB) extractions (Fig. 3B). Geochemical conditions in shallow groundwater (pH of 6–7, Fig. 5C; E$_h$ of 200–500 mV, Supplemental Fig. S4) are more favorable for precipitation of Fe oxides than Mn oxides by aerobic oxidation (equations 2 and 3, Table 1). The Fe(OH)$_3$ precipitate stability field covers about the upper right one-half of this range of pH and E$_h$ values, but no Mn solids stability fields fall within this range (Hem, 1985, p. 80 and 87). These results may partly explain generally lower Fe and consistently higher Mn concentrations in groundwater compared to stormwater (Figs. 4C and 5C, Supplemental Fig. S1). Due to the relatively low concentrations of Mn^{2+} and Fe^{2+} (typically less than 1000 μg L^{-1}; Fig. 5C) and only 2 and 1 electrons transferred, respectively, the contribution of Mn and Fe reduction toward the flow of electrons is minimal (Fig. 7B) and corresponding DOC consumption from these reactions alone would be small.

Interestingly, Fe concentrations were relatively high in some stormwater samples, including those that were oxic, and were often higher than groundwater Fe concentrations (Figs. 4C and 5C, Supplemental Fig. S1). This is probably caused by a combination of the following factors: (1) presence of colloidal Fe <0.45 μm in filtered samples, (2) complexation of Fe^{2+} with organic matter, (3) cyclic oxidation of Fe^{2+} and reduction of Fe^{3+}. First, Kennedy et al. (1974) report that fine particulates can pass through a 0.45 μm filter membrane, resulting in substantially overestimated "dissolved" Fe concentrations. These colloid-sized particles, if present, likely include Fe^{3+} precipitates given the oxic stormwater (equation 2, Table 1). A similar effect could be possible for groundwater samples, although given that SO$_4^{2-}$ reduction was observed, colloidal particles in groundwater

could potentially include both Fe^{2+} and Fe^{3+} precipitates (equations 14 and 15, Table 1). Second, organic matter present in the stormwater stored in the basin is likely to be of predominantly humic origin due to the submergence and subsequent decomposition of herbaceous vegetation during flooding. Stormwater Fe is positively correlated with stormwater TOC in the samples collected ($r^2 = 0.75$, $n = 10$), consistent with potential complexation with organic matter. Third, aerobic oxidation of Fe^{2+} may be inhibited when complexed with organic matter of humic origin, where the humic material effectively mediates a dynamic equilibrium between Fe^{2+} oxidation (equation 2, Table 1) and Fe^{3+} reduction (equation 13, Table 1) (Theis and Singer, 1974).

Complex interactions of the Mn and Fe cycles with the N and S cycles probably occur beneath the stormwater basin. Mn^{2+} and Fe^{2+} may serve as electron donors for autotrophic denitrification (equations 7 and 8, Table 1). But available data suggest that autotrophic denitrification, if it were occurring, probably was minor compared to heterotrophic denitrification. Based on the heterotrophic electron balance presented in Section 3.5.1 for the prolonged basin flooding in 2008, 3.0 mg kg^{-1} of FeS precipitated in the upper 1.9 m of soil (equations 14 and 16, Table 1), which is equivalent to an aqueous concentration of 11.6 mg L^{-1} (based on dry bulk density of 1.54 g cm^{-3} and porosity of 0.4 averaged from values reported by Naujock (2008) for the upper 1.4 m of soil). However, Fe^{2+} in this quantity of FeS can reduce only 0.37 mg L^{-1} NO_3^-–N, given the low ratio of electron acceptor to donor indicated by stoichiometry (equation 8, Table 1). Likewise, the highest measured Fe concentration of 558 µg L^{-1} (Fig. 5C) can reduce only 0.028 mg L^{-1} NO_3^-–N. Similar to Fe, oxidation of Mn^{2+} reduces relatively little NO_3^-, thus the highest measured Mn concentration of 2330 µg L^{-1} (0.5-m lysimeter, Fig. 6) can reduce only 0.23 mg L^{-1} NO_3^-–N (equation 7, Table 1). AAO extractable Fe oxide contents are typically above 1000 mg kg^{-1} (Fig. 3B) and likely are associated with Mn oxides, which, if subject to heterotrophic reduction (equations 12 and 13, Table 1), could yield increased Fe^{2+} and Mn^{2+} concentrations for autotrophic denitrification. However, the reduction of NO_3^- by Fe^{2+} or Mn^{2+} oxidation would cause a significant drop in pH, whereas a slight increase in pH occurred (Fig. 5C), suggesting limited Fe^{2+} and Mn^{2+} oxidation or pH buffering by dissolution of solid phase IC (Fig. 8).

3.5.5. Sulfate reduction

Cyclic variations in SO_4^{2-} concentrations in groundwater indicate that SO_4^{2-} reduction (equation 16, Table 1) was occurring beneath the basin (Fig. 5A). Water samples were not analyzed for H_2S, the end product of the reduction reaction, and no samples had a characteristic H_2S odor. However, H_2S can interact with Fe oxides to precipitate Fe sulfide minerals, consuming some or all H_2S produced (equations 14 and 15, Table 1) (Appelo and Postma, 2005). Additionally, H_2S generally dissociates to predominantly HS^- at pH <7 (Postma and Jakobsen, 1996). Despite the apparent dissolution of Fe oxides by reduction to Fe^{2+} (described in Section 3.5.4), the high Fe oxide contents of the soils are sufficient to serve in both roles (Fig. 3B), and simultaneous reduction of Fe oxides and SO_4^{2-} in subsurface sediments has been documented (Postma and Jakobsen, 1996). Increases

in SO_4^{2-} concentrations during periods of infrequent flooding (Fig. 5A) may be caused by oxidation of Fe sulfide minerals (equation 1, Table 1), and likely explains SO_4^{2-} concentrations in soil water and groundwater considerably higher than those of stormwater (Figs. 4A, 5A and 6; Supplemental Fig. S1). Compared to other electron acceptors, decreases in SO_4^{2-} concentration exceeding 5 mg L^{-1} are large (for example, during prolonged flooding periods of 2007 and 2008, Fig. 5A). These decreases combined with a transfer of 8 electrons indicate that SO_4^{2-} reduction accounts for the majority of the electron flow (Fig. 7B).

Reduced S in Fe sulfide minerals can serve as an electron donor for NO_3^- reduction, resulting in increases in SO_4^{2-} concentrations following decreases in NO_3^- concentration (equation 9, Table 1) (Postma et al., 1991), and may cause higher rates of denitrification than when coupled with C oxidation (Tesoriero and Puckett, 2011). Based on the heterotrophic electron balance presented in Section 3.5.1 for the prolonged basin flooding in 2008, 3.0 mg kg^{-1} of FeS precipitated in the upper 1.9 m of soil (equations 14 and 16, Table 1) could yield 4.1 mg kg^{-1} of FeS_2 (pyrite) via reduction of protons in H_2S (equation 18, Table 1). This quantity of FeS_2 (equivalent to an aqueous concentration of 15.8 mg L^{-1}) could reduce 5.2 mg L^{-1} NO_3^-–N (equation 9, Table 1). The actual FeS or pyrite content of the soils is unknown. X-ray diffraction analysis of clay and silt fractions of soils at the site did not detect the presence of pyrite, but detection limitations generally require quantities of at least 1–5% (W.G. Harris, personal communication, 2011). Lazareva (2004) reports that pyrite is commonly present in Miocene sediments (Hawthorn Group) in central Florida, which likely are similar to those at the study site, and note that H_2S produced during SO_4^{2-} reduction results in pyrite deposition. However, much of the FeS precipitated during previous basin flooding may be aerobically oxidized back to SO_4^{2-} (equation 1, Table 1) during intervening dry periods as suggested by increased SO_4^{2-} and DO concentrations in February and June 2008 (Fig. 5A). Additionally, decreases in NO_3^- do not coincide with increases in SO_4^{2-}, where stoichiometry indicates that 4.9 mg L^{-1} SO_4^{2-} is produced by reduction of 1 mg L^{-1} of NO_3^-–N (equation 9, Table 1). SO_4^{2-} and NO_3^- decreases were approximately concomitant (Figs. 5A and 7B) suggesting that S^- is not a dominant electron donor, which is consistent with precipitation of Fe sulfide minerals and the apparent absence of substantial H_2S. Continued increases in DIC (and CO_2) following NO_3^- depletion suggest that DOC is the predominant electron donor for SO_4^{2-} reduction (Fig. 7).

3.5.6. Methanogenesis

CH_4 concentrations in groundwater start to increase in August 2008 (Fig. 10A), lagging the Mn and Fe increases and SO_4^{2-} decreases (Fig. 5) as expected based on thermodynamic considerations (Appelo and Postma, 2005). CH_4 concentrations increase until peaking in November, and finally drop after the basin is dry again in December (Fig. 10A). Elevated CH_4 concentrations probably are the result of methanogenesis, typically the final step in biodegradation of organic matter under anoxic highly reducing conditions. The concurrent decreases in CO_2 and alkalinity when CH_4 peaks in November suggest use of the CO_2 reduction pathway for methanogenesis (equation 19, Table 1).

3.6. Cyclic variations in biogeochemical processes and effects on N cycling

The cyclic variations in biogeochemical processes generally coincided with wet and dry hydrologic conditions, with oxidizing conditions occurring in groundwater (Fig. 5A) at the beginning of wet periods upon the infiltration of aerobic stormwater (Fig. 4A). Anoxic conditions evolve in the shallow groundwater during prolonged flooding of the basin; low DO concentrations (less than 1 mg L^{-1}) continue during subsequent dry periods until the next major infiltration event (Fig. 5A). Therefore, cyclic hydrologic variations provide conditions amenable to the evolution of redox conditions, from oxic to methanic, and, combined with reaction kinetics and groundwater travel times, result in variable time scales for the TEAPs.

O_2 and NO_3^- reduction occurred at the shortest time scale, resulting in changes from oxic to anoxic groundwater (DO less than 0.3 mg L^{-1}) and NO_3^- depletion (NO_3^-–N less than 0.016 mg L^{-1}) within about 20 days (February–March 2008) and 40 days (June–July 2008) (Fig. 5A). However, the approximate monthly sampling interval was not sufficient to resolve these cyclic variations accurately. Cyclic variation in O_2 and NO_3^- concentrations at about a monthly time scale represents an approximate upper limit; higher frequency cycles probably occur. Isotopic data indicate enrichment of $\delta^{15}N[NO_3^-]$ and $\delta^{18}O[NO_3^-]$ within two days after infiltration at 0.9 and 1.4 m depths when NO_3^-–N was 1.8 and 3.3 mg L^{-1}, respectively (see 12-Jun-08 sample, Fig. 6). Because profile plots (Fig. 6) represent a snapshot in time, samples at discrete depths represent water recharged at different times, likely with different chemical compositions and experiencing different interactions during percolation through the unsaturated zone. Thus, NO_3^-–N would not necessarily be expected to decrease with depth. Isotopic fractionation suggests that the denitrification reaction was partially complete within two days.

Mn and Fe concentrations varied at a seasonal time scale, with increasing concentrations during prolonged flooding periods (summer and autumn) and decreasing concentrations during dry periods when flooding events were of shorter duration (winter and spring) (Fig. 5C). Only one and one-half cycles were observed during this study, however, and continued monitoring over several years would help confirm the persistence of these seasonal patterns.

Interestingly, cyclic variations in SO_4^{2-} concentrations in groundwater suggest that SO_4^{2-} reduction was more closely related to wet–dry cycles than Mn and Fe reduction. SO_4^{2-} reduction occurred not only during the prolonged summer and autumn flooding periods in 2007 and 2008, but also during the shorter flooding event in February–April 2008. SO_4^{2-} concentration in groundwater increased during the intervening dry periods. These cyclic variations are probably caused by the sensitivity of SO_4^{2-} reducing bacteria to O_2, such that when groundwater was oxic, SO_4^{2-} reduction was inhibited or confined to isolated anoxic sites in aquifer sediments.

Methanogenesis probably occurs at a seasonal time scale, as suggested by the gradual rise in CH_4 concentrations during the prolonged flooding period in 2008 and the absence of CH_4 in the shorter flooding period in March 2008. Only one-half cycle was observed, however, and, like Fe and Mn, continued

monitoring over several years would help confirm the persistence of this seasonal pattern. The relatively slow progression to methanic conditions is expected, given the need for less reductive TEAPs to occur first in order to largely deplete their respective electron acceptors.

Inference about biogeochemical reactions based on observed concentrations of redox reactants or products must be applied carefully. Only the net effects can be observed of potentially many simultaneous or coupled reactions occurring as stormwater infiltrates and percolates through the soil to the sampling point. Individual reactions could have occurred at shorter time scales and may have been observed had sampling frequency been increased, thus reaction rates driving elemental cycling at time scales shorter than the sampling frequency remain largely unknown at the study site. Additionally, biogeochemically active species can be affected by other physical or geochemical interactions. For example, Fe^{2+} can be produced by reduction of Fe oxide minerals as well as oxidation of Fe sulfide minerals (equations 9, 14 and 15, Table 1). Transport of dissolved gasses, such as N_2 and CH_4, can be significantly affected by gas/water phase interactions and bubble-mediated mass transfer (Geistlinger et al., 2010). The observed concentrations of any solute can be affected by differences in location of sampling relative to location of reaction, advective transport, and hydrodynamic dispersion. Temporal variations in excess N_2 concentrations in well PW may reflect some of these effects. Volumetric moisture content data indicate a gradual but prolonged rise in moisture content from early July through mid-September 2008 during continuous flooding of the basin (Fig. 2C). This phenomenon was most pronounced at the two shallowest TDR probes (0.3 and 0.6 m below the basin bottom) in 2008, but similar behavior was also apparent when the basin was flooded during summer 2009. These moisture content variations indicate the presence of a gas phase below the water table, likely attributable to air bubble entrapment and generation of subsurface biogenic gasses, such as CO_2, N_2 and CH_4 by OC oxidation, denitrification and methanogenesis. Bubble-mediated mass transfer of excess N_2 during transport from the depth of expected denitrification activity (0–1.4 m depth) to the screened depth of well PW (1.2–2.7 m) may have caused changes in concentration from the source depth to the sampling depth, resulting in attenuation of high-frequency variability. In the context of this conceptual model, the apparent seasonal pattern in excess N_2 concentrations may be brought about by such gas/water phase interactions, even though N_2 is being produced by denitrification at much shorter time scales. For example, the peak excess N_2 concentration in November 2008 (Fig. 10A) may have resulted from infiltration that occurred in June at the beginning of the summer wet season, as described in Section 3.5.3.1. Reactant and product concentrations in samples collected from well PW could also be affected by mixing of water from different depths and preferential flow pathways intersected by the 1.5-m-length well screen.

Water chemistry changes indicate a temporal succession of all TEAPs, from O_2 reduction to methanogenesis, in shallow groundwater beneath the stormwater infiltration basin (Figs. 5 and 6). The progression of biogeochemical conditions to Mn reduction and to even more highly reductive processes provides strong evidence that NO_3^-, when present, would

undergo reduction. The periodic introduction of additional NO_3^- electrons from infiltration of oxygenated stormwater redirects the flow of electrons from the more highly reductive processes to NO_3^- reduction, likely consisting of denitrification. The substantial transfer of electrons supported by these more highly reductive processes, particularly SO_4^{2-} reduction, implies that sufficient electron flow capacity is available to ensure denitrification would deplete all NO_3^-. For example, about 0.68 electron equivalents were transferred (excluding O_2 reduction) during the prolonged flooding of 2008 ($NO_3^- = 0.068$, Mn $= 0.026$, Fe $= 0.005$, $SO_4^{2-} = 0.580$; Fig. 7B), which is equivalent to 8.4 mg L^{-1} of NO_3^-–N. This probably represents a minimum NO_3^-–N that can be reduced, because higher frequency cycles were not discernible at the monthly sampling schedule. Also, observations during the study may underestimate the reductive potential of the system, which may respond even more dramatically if exposed to a greater flow of electron acceptors. Upon depletion of NO_3^- beneath the basin, more highly reductive conditions evolved and the sequential biogeochemical processes resumed. Thus biogeochemical cycling can effectively switch denitrification on and off, determining whether N fate is dominated by NO_3^- leaching or NO_3^- reduction.

4. Conclusions

A combination of hydrologic, soil chemistry, water chemistry, isotope and dissolved gas data was analyzed to assess denitrification and other biogeochemical processes occurring beneath a stormwater infiltration basin in a subtropical environment. Cyclic variations were present in many important redox sensitive constituents in the shallow groundwater system, including O_2, NO_3^-, Mn, Fe, SO_4^{2-}, CH_4 and DOC. These cyclic variations generally coincided with wet and dry hydrologic conditions, with oxidizing conditions occurring at the beginning of wet periods followed by reducing conditions.

Sequential biogeochemical processes following a thermodynamically governed and microbially mediated succession of TEAPs effectively determine whether the N cycle is limited to aerobic processes, which would generally result in NO_3^- leaching and downgradient groundwater contamination, or anoxic processes such as denitrification, which would decrease the N concentration in groundwater. Frequent and intense rainfall in humid, subtropical climates often cause prolonged flooding of stormwater infiltration basins. Under these conditions, results of this study indicate that TEAPs can progress to methanogenesis within a seasonal timescale during prolonged basin flooding, with O_2 and NO_3^- reduction occurring more quickly, within about one month or shorter time scale. Ammonification and nitrification probably occurred with the infiltration of oxygenated stormwater, but the subsequent progression of TEAPs inhibited these aerobic N cycle pathways. Water chemistry changes, isotopic fractionation, and excess N_2 generation indicate that denitrification was an important sink for N in this system. Soil chemistry results suggest that DNRA might be occurring to some degree and that anammox cannot be precluded. DOC provided by stormwater infiltration or a large solid-phase reservoir of OC probably served as the predominant electron donor for denitrification and other TEAPs. Denitrification occurs in the shallow soil zone at depths above 1.4 m as

suggested by enriched $\delta^{18}O[NO_3^-]$ and $\delta^{15}N[NO_3^-]$ (Figs. 6 and 11) as well as $\delta^{15}N[N_2]$ (Fig. 10B) progressively enriched during prolonged basin flooding, which likely is coupled with organic matter oxidation indicated by OC and IC concentrations from soil water extracts (Fig. 8) and lysimeters (Fig. 6). Some fraction of infiltrating stormwater probably is rapidly delivered to greater depths by macropores, largely bypassing the 0–1.4 m biogeochemically active zone, in a fashion similar to that described by Baram et al. (2012) in a clayey soil beneath a dairy waste lagoon. Excess N_2 produced in this zone subsequently could have been transported downward by the prevailing hydraulic gradient into the shallow groundwater where it was detected at concentrations up to 3 mg L^{-1} (Fig. 10A). Thus, anoxic groundwater and highly reducing conditions can occur cyclically beneath stormwater basins in subtropical environments and result in cyclic denitrification.

Results of this study indicate that NO_3^- contamination from stormwater infiltration basins can occur cyclically depending on the hydrologic conditions, effectively switching N fate from NO_3^- leaching to reduction in shallow groundwater. Such conditions should be considered when managing aquifer recharge from stormwater infiltration basins. Development of improved infiltration BMPs to mitigate NO_3^- impacts from stormwater infiltration basins could benefit from (1) further research on ways to replicate the biogeochemical conditions elucidated in this study that reduce N migration to groundwater and drinking water sources; and (2) greater application of subsurface biogeochemical cycling and redox chemistry to determine whether such N fate is controlled by conservative transport or reaction based processes. Improved BMPs could entail removal of native soil in the bottom of the stormwater basin and replacement with functionalized soil amendments (Hossain et al., 2010). O'Reilly et al. (2011) and Wanielista et al. (2011) report N losses beneath a stormwater infiltration basin incorporating such a BMP with functionalized soil amendments and attribute these losses to dilution, sorption, reduced nitrification, denitrification, or some combination of these processes.

Acknowledgments

Appendix A. Supplementary data

Supplementary data to this article can be found online at doi:10.1016/j.jconhyd.2012.03.005.

References

Aeschbach-Hertig, W., El-Gamal, H., Wieser, M., Palcsu, L., 2008. Modeling of excess air and degassing in groundwater by equilibrium partitioning with a gas phase. Water Resources Research 44, W08449.

Appelo, C.A.J., Postma, D., 2005. Geochemistry, Groundwater and Pollution, second ed. A.A. Balkema Publishers, Leiden, The Netherlands.

Arora, B., Mohanty, B.P., McGuire, J.T., 2011. Inverse estimation of parameters for multidomain flow models in soil columns with different macropore densities. Water Resources Research 47, W04512. doi:10.1029/2010WR009451.

Austin, A.T., Yahdjian, L., Stark, J.M., Belnap, J., Porporato, A., Norton, U., Ravetta, D.A., Schaeffer, S.M., 2004. Water pulses and biogeochemical cycles in arid and semiarid ecosystems. Oecologia 141, 221–235. doi:10.1007/s00442-004-1519-1.

Baker, L.A., 1992. Introduction to nonpoint source pollution in the United States and prospects for wetland use. Ecological Engineering 1, 1–26.

Baram, S., Kurtzman, D., Dahan, O., 2012. Water percolation through a clayey vadose zone. Journal of Hydrology 424–425, 165–171. doi:10.1016/j.jhydrol.2011.12.040.

Böhlke, J.K., 2002. Groundwater recharge and agricultural contamination. Hydrogeology Journal 10, 153–179 [erratum 10:438–439].

Böhlke, J.K., Wanty, R., Tuttle, M., Delin, G., Landon, M., 2002. Denitrification in the recharge area and discharge area of a transient agricultural nitrate plume in a glacial outwash sand aquifer, Minnesota. Water Resources Research 38 (7), 1105. doi:10.1029/2001WR000663.

Böhlke, J.K., Harvey, J.W., Voytek, M.A., 2004. Reach-scale isotope tracer experiment to quantify denitrification and related processes in a nitrate-rich stream, midcontinent United States. Limnology and Oceanography 49 (3), 821–838.

Böhlke, J.K., Smith, R.L., Miller, D.N., 2006. Ammonium transport and reaction in contaminated groundwater: application of isotope tracers and isotope fractionation studies. Water Resources Research 42, W05411. doi:10.1029/2005WR004349.

Brenton, R.W., Arnett, T.L., 1993. Methods of analysis by the U.S. Geological Survey National Water Quality Laboratory: determination of dissolved organic carbon by UV-promoted persulfate oxidation and infrared spectrometry. U.S. Geological Survey Open-File Report 92-480. USGS, Denver, CO.

Busenberg, E., Plummer, L.N., Bartholomay, R.C., 2001. Estimated age and source of the young fraction of ground water at the Idaho National Engineering and Environmental Laboratory. U.S. Geological Survey Water-Resources Investigations Report 01-4265 (DOE/ID-22177). USGS, Reston, VA.

Casciotti, K.L., Sigman, D.M., Hastings, M., Böhlke, J.K., Hilkert, A., 2002. Measurement of the oxygen isotopic composition of nitrate in seawater and freshwater using the denitrifier method. Analytical Chemistry 74, 4905–4912.

Chapelle, F.H., McMahon, P.B., Dubrovsky, N.M., Fujii, R.F., Oaksford, E.T., Vroblesky, D.A., 1995. Deducing the distribution of terminal electron-accepting processes in hydrologically diverse groundwater systems. Water Resources Research 31 (2), 359–371.

Cho, K.W., Song, K.G., Cho, J.W., Kim, T.G., Ahn, K.H., 2009. Removal of nitrogen by a layered soil infiltration system during intermittent storm events. Chemosphere 776, 690–696.

Clark, I.D., Fritz, P., 1997. Environmental Isotopes in Hydrogeology. CRC Press, Boca Raton, FL.

Clark, S.E., Pitt, R., 2007. Influencing factors and a proposed evaluation methodology for predicting groundwater contamination potential from stormwater infiltration activities. Water Environment Research 79 (1), 1–36.

Clark, I., Timlin, R., Bourbonnais, A., Jones, K., Lafleur, D., Wickens, K., 2008. Origin and fate of industrial ammonium in anoxic ground water—^{15}N evidence for anaerobic oxidation (anammox). Ground Water Monitoring & Remediation 28 (3), 73–82.

Clesceri, L.S., Greenberg, A.E., Eaton, A.D., 1998. Standard Methods for the Examination of Water and Wastewater, 20th ed. American Public Health Association, American Water Works Association, and Water Environment Federation, Washington, D.C.

Coats, K.H., Smith, B.D., 1964. Dead end pore volume and dispersion in porous media. Society of Petroleum Engineers Journal 4 (1), 73–84.

Coplen, T.B., 1988. Normalization of oxygen and hydrogen isotope data. Chemical Geology (Isotope Geoscience Section) 72, 293–297.

Coplen, T.B., 1994. Reporting of stable hydrogen, carbon, and oxygen isotopic abundances. Pure and Applied Chemistry 66, 273–276.

Coplen, T.B., Böhlke, J.K., Casciotti, K., 2004. Using dual-bacterial denitrification to improve delta ^{15}N determinations of nitrates containing mass-independent ^{17}O. Rapid Communications in Mass Spectrometry 18, 245–250.

Datry, T., Malard, F., Gibert, J., 2004. Dynamics of solutes and dissolved oxygen in shallow urban groundwater below a stormwater infiltration basin. Science of the Total Environment 329, 215–229.

Einsle, O., Kroneck, P.M.H., 2004. Structural basis of denitrification. Biological Chemistry 385, 875–883.

Epstein, S., Mayeda, T., 1953. Variation of O-18 content of water from natural sources. Geochimica et Cosmochimica Acta 4, 213–224.

Fisher, D., Charles, E.G., Baehr, A.L., 2003. Effects of storm water infiltration on quality of groundwater beneath retention and detention basins. Journal of Environmental Engineering 129 (5), 464–471. doi:10.1061/(ASCE)0733-9372(2003) 129:5(464.

Fishman, M.J. (Ed.), 1993. Methods of analysis by the U.S. Geological Survey National Water Quality Laboratory: Determination of inorganic and organic constituents in water and fluvial sediments. U.S. Geological Survey Open-File Rep. 93-125. USGS, Denver, CO.

Fishman, M.J., Friedman, L.C., 1989. Methods for determination of inorganic substances in water and fluvial sediments. U.S. Geological Survey Techniques of Water-Resources Investigations, Book 5, Chapter A1. USGS, Denver, CO.

Garbarino, J.R., Struzeski, T.M., 1998. Methods of analysis by the U.S. Geological Survey National Water Quality Laboratory—determination of elements in whole-water digests using inductively coupled plasma-optical emission spectrometry and inductively coupled plasma-mass spectrometry. U.S. Geological Survey Open-File Report 98-165. USGS, Denver, CO.

Garbarino, J.R., Kanagy, L.K., Cree, M.E., 2006. Determination of elements in natural-water, biota, sediment and soil samples using collision/reaction cell inductively coupled plasma-mass spectrometry. U.S. Geological Survey Techniques and Methods, Book 5, Sec. B, Chap.1. USGS, Denver, CO.

Geistlinger, H., Jia, R., Eisermann, D., Stange, C.F., 2010. Spatial and temporal variability of dissolved nitrous oxide in near-surface groundwater and bubble-mediated mass transfer to the unsaturated zone. Journal of Plant Nutrition and Soil Science 173, 601–609. doi:10.1002/jpln.200800278.

Green, C.T., Stonestrom, D.A., Bekins, B.A., Akstin, K.C., Schulz, M.S., 2005. Percolation and transport in a sandy soil under a natural hydraulic gradient. Water Resources Research 41, W10414. doi:10.1029/2005WR004061.

Green, C.T., Fisher, L.H., Bekins, B.A., 2008a. Nitrogen fluxes through unsaturated zones in five agricultural settings across the United States. Journal of Environmental Quality 37, 1073–1085.

Green, C.T., Pucket, L.J., Böhlke, J.K., Bekins, B.A., Phillips, S.P., Kauffman, L.J., Denver, J.M., Johnson, H.M., 2008b. Limited occurrence of denitrification in four shallow aquifers in agricultural areas of the United States. Journal of Environmental Quality 37, 994–1009.

Green, C.T., Böhlke, J.K., Bekins, B.A., Phillips, S.P., 2010. Mixing effects on apparent reaction rates and isotope fractionation during denitrification in a heterogeneous aquifer. Water Resources Research 46, W08525. doi:10.1029/2009WR008903.

Grossman, R.B., Reinsch, T.G., 2002. Bulk density and linear extensibility. In: Dane, J.H., Topp, G.C. (Eds.), Methods of Soil Analysis: Physical Methods, Part 4. Soil Science Society of America, Inc, Madison, WI.

Gu, C., Hornberger, G.M., Mills, A.L., Herman, J.S., Flewelling, S.A., 2007. Nitrate reduction in streambed sediments: effects of flow and biogeochemical kinetics. Water Resources Research 43, W12413. doi:10.1029/2007WR006027.

Hatt, B.E., Fletcher, T.D., Deletic, A., 2009. Hydrologic and pollutant removal performance of stormwater biofiltration systems at the field scale. Journal of Hydrology 365, 310–321.

Hem, J.D., 1985. Study and interpretation of the chemical characteristics of natural water, U.S. Geological Survey Water-Supply Paper 2254, third ed. USGS, Reston, VA.

Hoffman, G.L., Fishman, M.J., Garbarino, J.R., 1996. Methods of analysis by the U.S. Geological Survey National Water Quality Laboratory—in-bottle acid digestion of whole-water samples. U.S. Geological Survey Open-File Report 96-225. USGS, Denver, CO.

Hossain, F., Chang, N., Wanielista, M., 2010. Modeling kinetics and isotherms of functionalized filter media for nutrient removal from stormwater dry ponds. Environmental Progress & Sustainable Energy 29, 319–333. doi:10.1002/ep. 10415.

Kahl, J.S., Norton, S.A., Fernandez, I.J., Nadelhoffer, K.J., Driscoll, C.T., Aber, J.D., 1993. Experimental inducement of nitrogen saturation at the watershed scale. Environmental Science and Technology 27, 565–568.

Katz, B.G., 1992. Hydrochemistry of the Upper Floridan aquifer. Florida: U.S. Geological Survey Water-Resources Investigations Report 91-4196. USGS, Tallahassee, FL.

Katz, B.G., 2004. Sources of nitrate contamination and age of water in large karstic springs of Florida. Environmental Geology 46, 689–706.

Katz, B.G., Hornsby, H.D., Böhlke, J.F., Mokray, M.F., 1999. Sources and chronology of nitrate contamination in spring waters, Suwannee River basin, Florida. U.S. Geological Survey Water-Resources Investigations Report 99-4252. USGS, Tallahassee, FL.

Katz, B.G., Sepulveda, A.A., Verdi, R.J., 2009. Estimating nitrogen loading to ground water and assessing vulnerability to nitrate contamination in a large karstic springs basin. Journal of the American Water Resources Association 45 (3), 607–627.

Katz, B.G., Griffin, D.W., McMahon, P.B., Harden, H.S., Wade, E., Hicks, R.W., Chanton, J.P., 2010. Fate of effluent-borne contaminants beneath septic tank drainfields overlying a karst aquifer. Journal of Environmental Quality 39 (4), 1181–1195. doi:10.2134/jeq2009.0244.

Kendall, C., 1998. Tracing nitrogen sources and cycling in catchments. In: Kendall, Carol, McDonnell, J.J. (Eds.), Isotope Tracers in Catchment Hydrology. Elsevier, Amsterdam, The Netherlands, pp. 519–576.

Kendall, C., Aravena, R., 2000. Nitrate Isotopes in Groundwater Systems. In: Cook, P.G., Herczeg, A.L. (Eds.), Environmental tracers in subsurface hydrology. Kluwer Academic Publishers, Boston, MA, pp. 261–297.

Kennedy, V.C., Zellweger, G.W., Jones, B.F., 1974. Filter pore-size effects on the analysis of Al, Fe, Mn, and Ti in water. Water Resources Research 10 (4), 785–790.

Kim, H., Seagren, E.A., Davis, A.P., 2003. Engineered bioretention for removal of nitrate and stormwater runoff. Water Environment Research 75 (4), 355–367.

Knowles Jr., L., Katz, B.G., Toth, D.J., 2010. Using multiple chemical indicators to characterize and determine the age of groundwater from selected vents of the Silver Springs Group, central Florida, USA. Hydrogeology Journal 18, 1825–1838.

Kurtzman, D., Scanlon, B.R., 2011. Groundwater recharge through Vertisols— irrigated cropland versus natural land, Israel. Vadose Zone Journal 10 (2), 662–674. doi:10.2136/vzj2010.0109.

Lazareva, O., 2004. Detailed geochemical and mineralogical analyses of naturally occurring arsenic in the Hawthorn Group. M.Sc. Thesis, University of Florida, Gainesville, FL.

Maddox, G.L., Lloyd, J.M., Scott, T.M., Upchurch, S.B., Copeland, R., 1992. Florida's groundwater quality monitoring program—background hydrochemistry. Special Publication, 34. Florida Geological Survey, Tallahassee, FL.

Mahmood, T., Ali, R., Malik, K.A., Aslam, Z., Ali, S., 2005. Seasonal pattern of denitrification under an irrigated wheat-maize cropping system fertilized with urea and farmyard manure in different combinations. Biology and Fertility of Soils 42 (1), 1–9.

Mariotti, A., 1983. Atmospheric nitrogen is a reliable standard for natural ^{15}N abundance measurements. Nature 303, 685–687.

McMahon, P.B., Chapelle, F.H., 2007. Redox processes and water quality of selected principal aquifer systems. Ground Water 46, 259–271. doi:10.1111/j.1745-6584.2007.00385.x.

Mecikalski, J.R., Sumner, D.M., Jacobs, J.M., Pathak, C.S., Paech, S.J., Douglas, E.M., 2011. Use of visible geostationary operational meteorological satellite imagery in mapping reference and potential evapotranspiration over Florida. In: Labedzki, L. (Ed.), Evapotranspiration. InTech Publishers, Vienna, Austria.

National Climate Data Center, 2011. NNDC Climate Data Online[accessed May 2011] http://cdo.ncdc.noaa.gov/cgi-bin/cdo/cdostnsearch.pl.

Naujock, L.J., 2008. Development of hydraulic and soil properties for soil amendments and native soils for retention ponds in Marion County, Florida. M.Sc. Thesis, University of Central Florida, Orlando, FL.

Norman, R.J., Stucki, J.W., 1981. The determination of nitrate and nitrite in soil extracts by ultraviolet spectrophotometry. Soil Science Society of America Journal 45, 347–353.

O'Reilly, A.M., 1998. Hydrogeology and simulation of the effects of reclaimed-water application in west Orange and southeast Lake Counties, Florida. U.S. Geological Survey Water-Resources Investigations Report 97-4199. USGS, Tallahassee, FL.

O'Reilly, A.M., Chang, N.B., Wanielista, M.P., 2007. Data mining analysis of nitrate occurrence in ground water in central and northeast Florida and an overview of stormwater best management practices for nitrate control. Proceedings 9th Biennial Stormwater Research and Watershed Management Conference, Orlando, FL. May 2–3, 2007. University of Central Florida Stormwater Management Academy, Orlando, FL.

O'Reilly, A.M., Chang, N.B., Wanielista, M.P., Xuan, Z., 2011. Identifying biogeochemical processes beneath stormwater infiltration ponds in support of a new best management practice for groundwater protection. In: Schirmer, M., Hoehn, E., Vogt, T. (Eds.), GQ10: Groundwater Quality Management in a Rapidly Changing World, Proc. 7th International Groundwater Quality Conference, Zurich, Switzerland, 13–18 June 2010. IAHS Publ., 342. IAHS Press, Oxfordshire, United Kingdom, pp. 437–440.

Pachepsky, Ya.A., Ivanova, S.A., Korsunskaya, L.P., Polubesova, T.A., 1994. Adsorption of Cl^-, NO_3^-, and SO_4^{2-} anions by krasnozem. Agrochimica 38 (5–6), 305–314.

Page, D., Dillon, P., Vanderzalm, J., Toze, S., Sidhu, J., Barry, K., Levett, K., Kremer, S., 2010. Risk assessment of aquifer storage transfer and recovery with urban stormwater for producing water of a potable quality. Journal of Environmental Quality 39, 2029–2039.

Patton, C.J., Kryskalla, J.R., 2003. Methods of analysis by the U.S. Geological Survey National Water Quality Laboratory—evaluation of alkaline persulfate digestion as an alternative to Kjeldahl digestion for determination of total and dissolved nitrogen and phosphorus in water. U.S. Geological Survey Water-Resources Investigations Report 03-4174. USGS, Denver, CO.

Peterjohn, W.T., Adams, M.B., Gilliam, F.S., 1996. Symptoms of nitrogen saturation in two central Appalachian hardwood forest ecosystems. Biogeochemistry 35, 507–522.

Phelps, G.G., 2004. Chemistry of ground water in the Silver Springs basin, Florida, with emphasis on nitrate. U.S. Geological Survey Scientific Investigations Report 2004-5144. USGS, Tallahassee, FL.

Phelps, G.G., Walsh, S.J., Gerwig, R.M., Tate, W.B., 2006. Characterization of the hydrology, water chemistry, and aquatic communities of selected springs in the St. Johns River Water Management District, Florida, 2004. U.S. Geological Survey Open-File Report 2006-1107. USGS, Tallahassee, FL.

Pitt, R., Clark, S., Field, R., 1999. Groundwater contamination potential from stormwater infiltration practices. Urban Water 1, 217–236.

Postma, D., Jakobsen, R., 1996. Redox zonation: equilibrium constraints on the Fe(III)/SO4-reduction interface. Geochimica et Cosmochimica Acta 60 (17), 3169–3175.

Postma, D., Boesen, C., Kristiansen, H., Larsen, F., 1991. Nitrate reduction in an unconfined sandy aquifer: water chemistry, reduction processes, and geochemical modeling. Water Resources Research 27 (8), 2027–2045.

Professional Service Industries, Inc. (Jammal and Associates Division, 1993. Full-scale hydrologic monitoring of stormwater retention ponds and recommended hydro-geotechnical design methodologies. St. Johns River Water Management District Special Publication SJ93-SP10. SJRWMD, Palatka, FL.

Révész, K., Casciotti, K., 2007. Determination of the delta ($^{15}N/^{14}N$) and delta ($^{18}O/^{16}O$) of nitrates in water: RSIL Lab Code 2900. In: Révész, K., Coplen, T.B. (Eds.), Methods of the Reston Stable Isotope Laboratory. U.S. Geological Survey Techniques and Methods, Book 10, Sec. C, Chap. 17. USGS, Reston, VA.

Révész, K., Coplen, T.B., 2008. Determination of the delta ($^{18}O/^{16}O$) of water: RSIL lab code 489. In: Révész, K., Coplen, T.B. (Eds.), Methods of the Reston Stable Isotope Laboratory. U.S. Geological Survey Techniques and Methods, Book 10, Sec. C, Chap. 17. USGS, Reston, VA.

Schiffer, D.M., 1989. Effects of three highway-runoff detention methods on water quality of the surficial aquifer system in central Florida. U.S. Geological Survey Water-Resources Investigations Report 88-4170. USGS, Tallahassee, FL.

Schulze, D.G., 2002. An introduction to soil mineralogy. In: Dixon, J.B., Schulze, D.G. (Eds.), Soil Mineralogy with Environmental Applications. Soil Sci. Soc. Am, Madison, WI, pp. 1–35.

Sexstone, A.J., Parkin, T.B., Tiedje, J.M., 1985. Temporal response of soil denitrification rates to rainfall and irrigation. Soil Science Society of America Journal 49, 99–103.

Sigman, D.M., Casciotti, K.L., Andreani, M., Barford, C., Galanter, M., Böhlke, J.K., 2001. A bacterial method for the nitrogen isotopic analysis of nitrate in seawater and freshwater. Analytical Chemistry 73, 4145–4153.

St. Johns River Water Management District, 2010. Springs of the St. Johns River Water Management District[accessed October 2010] http://www.sjrwmd.com/springs/index.html.

Struzeski, T.M., DeGiacomo, W.J., Zayhowski, E.J., 1996. Methods of analysis by the U.S. Geological Survey National Water Quality Laboratory—determination of dissolved aluminum and boron in water by inductively coupled plasma-atomic emission spectrometry. U.S. Geological Survey Open-File Report 96-149. USGS, Denver, CO.

Sumner, D.M., Bradner, L.A., 1996. Hydraulic characteristics and nutrient transport and transformation beneath a rapid infiltration basin, Reedy Creek

Improvement District, Orange County, Florida. U.S. Geological Survey Water-Resources Investigations Report 95-4281. USGS, Tallahassee, FL.

Taylor, G.D., Fletcher, T.D., Wong, T.H.F., Breen, P.F., Duncan, H.P., 2005. Nitrogen composition in urban runoff—implications for stormwater management. Water Research 39, 1982–1989. doi:10.1016/j.watres.2005.03.022.

Tesoriero, A.J., Puckett, L.J., 2011. O_2 reduction and denitrification rates in shallow aquifers. Water Resources Research 47, W12522. doi:10.1029/2011WR010471.

Theis, T.L., Singer, P.C., 1974. Complexation of iron(II) by organic matter and its effect on iron(II) oxygenation. Environmental Science and Technology 8 (6), 569–573.

Thomas, B.P., Law, L., Stankey, D.L., 1979. Soil survey of Marion County, Florida. U.S. Department of Agriculture, Soil Conservation Service, Washington D.C.

Tobias, C.R., Böhlke, J.K., Harvey, J.W., 2007. The oxygen-18 isotope approach for measuring aquatic metabolism in high-productivity waters. Limnology and Oceanography 52, 1439–1453.

U.S. Environmental Protection Agency, 2005. Ecosystem stress from chronic exposure to low-levels of nitrate. EPA 600/R-05/087, October 2005. U.S. Environmental Protection Agency, Washington, DC.

U.S. Environmental Protection Agency, 2011. Water quality standards for the State of Florida's lakes and flowing waters; Proposed Rule, Federal Register vol. 75, no. 16, Tuesday, January 26, 2010[accessed May 2011] http://edocket.access.gpo.gov/2010/pdf/2010-1220.pdf.

U.S. Geological Survey, 1998. National field manual for the collection of water quality data. U.S. Geological Survey Techniques of Water-Resources Investigations, Book 9, Chapters A1–A9. USGS, Reston, VA. Also available at http://water.usgs.gov/owq/FieldManual/.

U.S. Geological Survey, 2011a. Florida potential and reference evapotranspiration 1995–2004[accessed May 2011] http://hdwp.er.usgs.gov/et.asp.

U.S. Geological Survey, 2011b. Florida potential and reference evapotranspiration 2005–2010[accessed May 2011] http://hdwp.er.usgs.gov/et2005-2010.asp.

Vitousek, P.M., Aber, J., Howarth, R.W., Likens, G.E., Matson, P.A., Schindler, D.W., Schlesinger, W.H., Tilman, G.D., 1997. Human alteration of the global nitrogen cycle: causes and consequences. Ecological Applications 7, 737–750.

Vogel, J.C., Talma, A.S., Heaton, T.H.E., 1981. Gaseous nitrogen as evidence for denitrification in ground water. Journal of Hydrology 50, 191–200.

Walkley, A., Black, I.A., 1934. An examination of Degtjareff method for determining soil organic matter and a proposed modification of the chromic acid titration method. Soil Science 37, 29–38.

Walsh, S.J., Knowles Jr., L., Katz, B.G., Strom, D.G., 2009. Hydrology, water quality, and aquatic communities of selected springs in the St. Johns River Water Management District, Florida. U.S. Geological Survey Scientific Investigations Report 2009-5046. USGS, Tallahassee, FL.

Wanielista, M., Kersten, R., Eaglin, R., 1997. Hydrology: Water Quantity and Quality Control, second ed. John Wiley, New York.

Wanielista, M.P., Chang, N.B., Naujock, L.J., Xuan, Z., Biscardi, P.G., 2011. Nitrogen transport and transformation beneath stormwater retention basins in karst areas and effectiveness of stormwater best management practices for reducing nitrate leaching to ground water. Final Report. Stormwater Management Academy, University of Central Florida, Orlando, FL. October.

Ward, M.H., deKok, T.M., Levallois, P., Brender, J., Gulis, G., Nolan, B.T., VanDerslice, J., 2005. Workgroup report: drinking-water nitrate and health—recent findings and research needs. Environmental Health Perspectives 113, 1607–1614. doi:10.1289/ehp. 8043.

Weiss, R.F., 1970. The solubility of nitrogen, oxygen, and argon in water and seawater. Deep Sea Research 17, 721–735.

Weitz, A.M., Linder, E., Frolking, S., Crill, P.M., Keller, M., 2001. N_2O emissions from humid tropical agricultural soils: effects of soil moisture, texture and nitrogen availability. Soil Biology and Biochemistry 33, 1077–1093.

Wilde, F.D., Radtke, D.B., 1998. Field measurements. National field manual for the collection of water-quality data: U.S. Geological Survey Techniques of Water-Resources Investigations, Book 9, Chap. A6.

Zubair, A., Hussain, A., Farooq, M.A., Abbasi, H.N., 2010. Impact of storm water on groundwater quality below retention/detention basins. Environmental Monitoring and Assessment 162, 427–437. doi:10.1007/s10661-009-0807-y.